ITERATION PROCEDURE FOR SUDDEN LOCAL ALTERATION OF STRUCTURAL STIFFNESS

Bruce Forde

University of British Columbia

Vancouver, Canada

Mitteilungen Nr. 6 (1986)

Institut für Baustatik der Universität Stuttgart

Professor Dr.-Ing. E. Ramm

Stuttgart 1986

Berichte des Instituts für Baustatik sind die ausführliche Dokumentation abgeschlossener Forschungsvorhaben.

Mitteilungen des Instituts für Baustatik stellen Auszüge und ergänzende Informationen aus dem Arbeitsgebiet des Instituts dar.

Die Erscheinungsfolge ist zwanglos.

Berichte und Mitteilungen können über das Institut für Baustatik der Universität Stuttgart, Pfaffenwaldring 7, 7000 Stuttgart 80, bezogen werden.

VORWORT

Der vorliegende Institutsbericht wurde von Herrn Bruce Forde, M.Sc., während seines einjährigen Studienaufenthaltes am Institut für Baustatik an der Universität Stuttgart angefertigt. Im Vordergrund seiner Tätigkeit stand neben der Entwicklung eines nichtlinearen Fachwerkelements die Untersuchung von Iterationsverfahren zur Berechnung von Tragstrukturen mit Hilfe der finiten Elementmethode. Insbesondere sind mit dem Computerprogramm NISA die von Ramm vorgeschlagenen und von Schweizerhof weiterentwickelten Kurvenverfolgungsalgorithmen zusammen mit den Quasi - Newton - Verfahren auf Tragsysteme mit extrem veränderlichem Strukturverhalten angewendet worden.

Besonderer Dank gilt dem Deutschen Akademischen Austauschdienst für seine bereitwillige finanzielle Förderung von Herrn Forde.

Abstract

This report is divided into three parts:

1. Path following methods in nonlinear finite element analysis.
2. Explicit derivation of stiffness expressions for space truss elements.
3. Numerical analysis of extremely nonlinear problems.

A family of arc length methods is derived using orthogonality principles. These methods are theoretically compared in terms of computational efficiency and convergence characteristics. Descriptions are given for the common quasi Newton updates along with comments on the satisfaction of the quasi Newton equations for use in conjunction with arc length procedures.

Derivations of the stiffness expressions for space truss elements in elastic, plastic and post buckled configurations are given in explicit forms. The implementation of this element in NISA80 is documented with descriptions of the modules used for arc length and quasi Newton updates.

Solutions for test problems are given to establish the validity of results from the space truss elements. Some small extremely nonlinear problems are used to identify the limitations of the path following methods. Additional large nonlinear problems are used to rank the various path following procedures in terms of computational efficiency.

Contents

Notation

^{m}L = Length
^{m}A = Cross sectional area
I = Moment of Inertia
r = Radius of gyration
c = Distance to the outer fiber from the neutral axis
η = Effective slenderness ratio factor

$^{m}\sigma$ = Cauchy axial stress
σ = Stress increment
$^{E}\sigma$ = Euler buckling axial stress
f = Post-buckling axial stress amplification factor

$^{m}\epsilon$ = Engineering axial strain
ϵ = Axial strain increment
$^{m}\hat{e}$ = Post-buckling effective axial strain

$^{m}\mathbf{x}$ = Total displacement vector
$\mathbf{u}^{(i)}$ = Incremental displacement vector
$\Delta\mathbf{u}$ = Total change in $\mathbf{u}$
$\Delta\mathbf{u}^{I}$ = Change in $\mathbf{u}$ for $\Delta\lambda = 1$
$\Delta\mathbf{u}^{II}$ = Change in $\mathbf{u}$ due to the unbalanced load vector
$^{m}\delta$ = Post-buckling effective axial displacement
$^{m}\Delta$ = Post-buckling transverse displacement at midspan

$\mathbf{P}$ = Reference external load vector
$\mathbf{F}^{(i)}$ = Internal force vector
$\mathbf{R}^{(i)}$ = External load vector $\equiv {}^{m}\lambda\mathbf{P}$
$-\mathbf{G}^{(i)}$ = Unbalanced load vector $\equiv \mathbf{R}^{(i)} - \mathbf{F}^{(i)}$
$^{m}\lambda$ = Total load factor
$\lambda^{(i)}$ = Incremental load factor
$\Delta\lambda$ = Change in $\lambda^{(i)}$
β = Scale factor for arc length procedures
^{m}S = Axial force
^{E}S = Euler buckling axial load

$\mathbf{K}^{(i)}$ = Tangent stiffness vector
$\mathbf{t}^{(i)}$ = Tangent vector
$\mathbf{n}^{(i)}$ = Normal vector
$\mathbf{r}^{(i)}$ = Residual vector
$t^{(i)}$ = Length of tangent vector
$R^{(i)}$ = Residual scalar
s = Arc length

$\mathbf{v}^{(i)}$ = Unbalanced load vector
$\Delta\mathbf{v}^{(i)}$ = Change in unbalanced load vector
$\mathbf{w}^{(i)}$ = Quasi Newton update vector
$\alpha^{(i)}$ = Quasi Newton update factor (rank 1)
$\beta^{(i)}$ = Quasi Newton update factor (rank 2)

References

[1] Britvec, S.J. (1973) "The Stability of Elastic Systems", Pergamon Press, New York.

[2] Broyden, C.G. (1970) "The convergence of a class of double-rank minimisation algorithms, 1: general considerations, and 2: the new algorithm", Journal Institute of Mathematical Applications, Vol. 6, 76-90, and 222-231.

[3] Byrd, R.F. and Friedman, M.D. (1971) "Handbook of Elliptic Integrals for Engineers and Scientists", Springer, Berlin.

[4] Chu, K.H. and Rampetsreiter, R.H. (1972) "Large deflection buckling of space frames", Journal of the Structural Division, A.S.C.E., Vol. 98, 2701-2722.

[5] Crisfield, M.A. (1981) "A Fast Incremental/Iterative Solution Procedure that Handles Snap Through", Computers and Structures, Vol. 13, 55-62.

[6] Davidon, W.C. (1959) "Variable Metric Method for Minimisation", Research and Development Report, A.N.L. 5990, Argonne National Laboratory, Illinois.

[7] Fletcher, R. and Powell, M.J.D. (1963) "A rapidly convergent method for minimisation", Computer Journal, Vol. 6, 163-168.

[8] Fletcher, R. (1970) "A new approach to variable metric algorithms", Computer Journal, Vol 13, 317-322.

[9] Geradin, M., Idelsohn, S. and Hogge, M. (1981) "Computational strategies for the solution of large nonlinear problems via Quasi-Newton methods", Computers and Structures, Vol. 13, 73-81.

[10] Goldfarb, D. (1970) "A family of variable metric methods derived by variational means", Mathematical Computations, Vol. 24, 23-26.

[11] Jagannathan, D.S., Epstein, H.I. and Christiano, P. (1975) "Nonlinear analysis of reticulated space trusses", Journal of the Structural Division, ASCE, Vol. 101 (ST12) 2641-2658.

[12] Kondoh, K. and Atluri, S.N. (1985) "Influence of Local Buckling on Global Instability: Simplified, Large Deformation, Post-Buckling Analyses of Plane Trusses", Computers and Structures, Vol. 21, 613-627.

[13] Matthies, H. and Strang, G. (1979) "The Solution of Nonlinear Finite Element Equations", International Journal of Numerical Methods in Engineering, Vol. 14, 1613-1626.

[14] Papadrakakis, M. (1981) "Post-buckling analysis of spatial structures by vector iteration methods", Computers and Structures, Vol. 14, 393-402.

[15] Paradiso, M., Reale, E. and Tempesta, G. (1979) "Nonlinear post-buckling analysis of reticulated dome structures", Proceedings IASS World Congress on Shell and Spatial Structures, Madrid.

[16] Powell, G. and Simons, J. (1981) "Improved iteration strategy for non-linear structures", International Journal of Numerical Methods in Engineering, Vol. 17, 1455-1467.

[17] Ramm, E. (1980) "Strategies for Tracing the Nonlinear Response Near Limit Points", Europe-U.S. Workshop, Nonlinear finite element analysis in structural mechanics, Ruhr-Universität Bochum, Germany. Editors: W. Wunderlich, E. Stein, and K.J. Bathe.

[18] Riks, E. (1972) "The Application of Newton's Method to the Problem of Elastic Stability", Journal of Applied Mechanics, Vol.39,1060-1066.

[19] Rosen, A. and Schmit (1979) "Design oriented analysis of imperfect truss structures", International Journal of Numerical Methods in Engineering, Vol. 14, 1309-1321.

[20] Schweizerhof, K. and Wriggers, P. (1986) "Consistent linearization for path following methods in nonlinear FE analysis", Accepted for publication in Computer Methods in Applied Mechanics and Engineering.

[21] Schweizerhof, K. and Ramm, E. (1986) "Combining Quasi-Newton and Arc-Length Methods for the Analysis of Nonlinear Problems in the Postlimit Range", Submitted to The First World Congress on Computational Mechanics, Austin, Texas, September 1986.

[22] Shanno, D.F. (1970) "Conditioning of quasi-Newton methods for functional minimisation", Mathematical Computations, Vol. 24, 647-656.

[23] Tan, Hoon Swee (1985) "Finite Element Analysis of the Elastic, Non-Linear Response of Frames, Plates and Arbitrary Shells to Static Loads", PhD Thesis, Department of Civil Engineering, University of Queensland.

[24] Thompson, J.M.T. and Hunt, G.W. (1973) "A General Theory of Elastic Stability", Wiley, New York.

[25] Timoshenko, S.P. and Gere, J.M. (1961) "Theory of Elastic Stability", 2nd Edition, McGraw-Hill, New York, 76-82.

[26] Wempner, G.A. (1971) "Discrete Approximations Related to Nonlinear Theories of Solids", International Journal of Solids Structures, Vol. 7, 1581-1599.

[27] Zhu, Runxiang and Parisch, H. (1982) "A Study of the Different Solution Methods for Nonlinear Problems", Institut für Statik und Dynamik der Luft- und Raumfahrtkonstruktionen, ISD Report No. 304, Universität Stuttgart.

Acknowledgements

I would like to thank the Deutscher Akademischer Austauschdienst (DAAD) for the financial support made available to me in the form of a research scholarship. I am also indebted to the following people:

Prof. Dr.-Ing. E. Ramm - for his guidance and direction.

Dr.-Ing. P. Osterrieder - for his reinforcement of ideas.

Dr.-Ing. K. Schweizerhof - for sharing his momentum.

Dipl.-Ing. A. Matzenmiller - for his helpful discussions.

Frau D. Tao, B.E. - for her constant involvement.

Fräulein E. Lee, B.Sc. - for her patience and encouragement.

Additional thanks are owed to the members of the Institut für Baustatik for bearing with me while I was learning the German language.

1. Introduction

Iterative solution of the nonlinear equations found in finite element analysis is a classical theme found in academia. The practical implementation of path following procedures into computationally effective schemes is of more interest to the professional community. This report investigates the theoretical performance of some experimental iteration procedures to provide a useful classification of the applicability of such procedures in the solution of the problems found in engineering practice.

1.1 Application of Literature

The arc length methods suggested by Riks[18], Wempner [26], Ramm [17], Schweizerhof/Wriggers [20], and Crisfield [5] are theoretically and numerically compared. Quasi Newton updates of Broyden [2], Davidon [6], Fletcher/Powell [7], Goldfarb [10], and Shanno [22] with various matrix and vector formulations of these updates from Geradin/Idelsohn/Hogge [9], Matthies/Strang [13], and Schweizerhof/Ramm [21] are utilized to improve the computational behaviour of the path following procedures.

1.2 Objectives and Scope

A simple space truss element is developed for use in nonlinear analysis. The elastic, plastic, and buckling phenomena representable with this element provide extremely variable local stiffness response. Typical behaviour of reticulated shell structures modelled with this element involves potential sudden local alteration of global stiffness. This presents difficulty for most solution procedures and is used to rank the methods in terms of computational efficiency.

A series of extremely nonlinear problems are chosen to test both the ability of the element to correctly model complex structural behaviour and the ability of the solution procedures to follow the load/displacement path. A comprehensive numerical study of the implemented arc length and quasi Newton procedures completes the project by providing results which identify the efficiency of the various schemes in practical applications.

2. Nonlinear Path Following Methods

A variety of strategies are available for tracing the load/displacement response of structures subjected to ultimate loads. Analyses which utilize load or displacement control may fail to converge in the area of limit points for problems with snap-through or snap-back phenomena (Figure 2.1). Since the postcritical behaviour is often related to the imperfection sensitivity of a structure, the prediction of response in this area may be of great value [17]. Consequently, nonlinear finite element programs should have the ability to follow the structural response into the postcritical range.

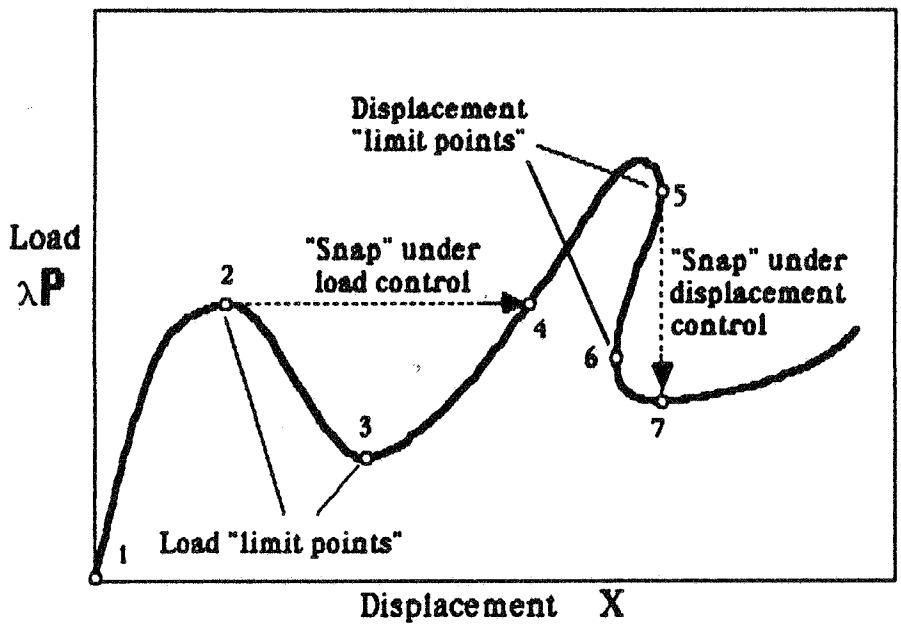

Figure 2.1 Load/Displacement Path [5].

In this report, variations of the arc length procedure of Riks [18] and Wempner [26] are combined with quasi Newton methods for path following in the vicinity of limit points. Quasi Newton methods are used with arc length procedures to accelerate convergence without incurring the expensive computations associated with the pure Newton method.

2.1 Arc Length Methods

The general goal of all arc length procedures is the control of iteration in the load/displacement space so that a complex path can be followed well into the postcritical range. The ideal procedure is one that has a strong domain of attraction which provides consistent convergence in the vicinity of limit points. A compromise must be made between this ideal and a numerically efficient scheme. Both simple and complex formulations have been developed in the literature each with their own merits. Some of these methods are derived here and then theoretically compared.

The fundamental theorem of variational analysis leads to the standard finite element equibrium equations.

$$\lambda \mathbf{P} - \mathbf{F}(\mathbf{x}) = \mathbf{0} \tag{2.1}$$

A classical Newton scheme provides an incremental iterative solution.

$$\mathbf{K}^{(i)} \Delta \mathbf{u} = \lambda \mathbf{P} - \mathbf{F}(\mathbf{x}^{(i)}) \tag{2.2}$$

$$\mathbf{x}^{(i+1)} = \mathbf{x}^{(i)} + \Delta \mathbf{u} \tag{2.3}$$

The proportional loading factor λ must be written in incremental form for application with arc length procedures. This yields a general formulation.

$$\mathbf{K}^{(i)} \Delta \mathbf{u} - \mathbf{P} \Delta \lambda = ({}^{m}\lambda + \lambda^{(i)}) \mathbf{P} - \mathbf{F}(\mathbf{x}^{(i)}) = -\mathbf{G}^{(i)} \tag{2.4}$$

$$\mathbf{x}^{(i+1)} = {}^{m}\mathbf{x} + \mathbf{u}^{(i)} + \Delta \mathbf{u} \tag{2.5}$$

The incremental displacement can be written in two components. The first is the displacement $\Delta \mathbf{u}^{I}$ due to a unit load factor multiplied by the incremental variation in the load level $\Delta\lambda$. The second is the displacement update for a conventional "load controlled" Newton procedure due to the unbalanced loads $\mathbf{G}^{(i)}$.

$$\Delta \mathbf{u} = \Delta \mathbf{u}^{I} \Delta \lambda + \Delta \mathbf{u}^{II} \tag{2.6}$$

$$\Delta \mathbf{u}^{I} = \mathbf{K}^{-1} \mathbf{P} \tag{2.7}$$

$$\Delta \mathbf{u}^{II} = -\mathbf{K}^{-1} \mathbf{G}^{(i)} \tag{2.8}$$

The relationship between these components in the load/displacement space is displayed in figure 2.2.

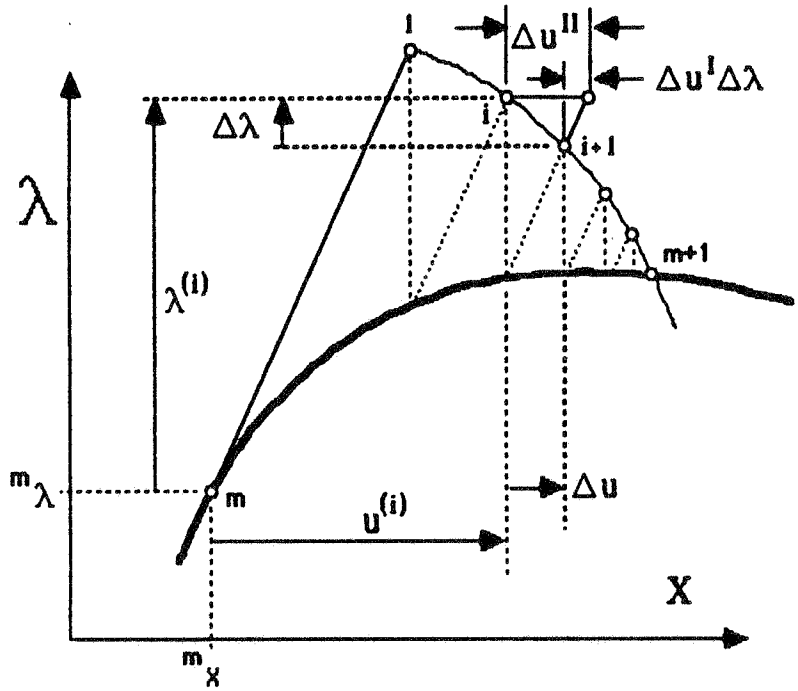

Figure 2.2 Generalized Incremental Formulation.

This procedure can be interpreted as either a modified Newton, quasi Newton, or pure Newton iteration scheme. Using this notation, a family of arc length methods with a variety of update directions can be derived.

2.1.1 Orthogonal Plane Methods

A general formulation for arc length procedures can be derived from orthogonality principles. An arbitrary update direction can be defined in terms of an assumed vector $\mathbf{n}^{(i)}$. The requirements for this update vector can be satisfied through the reference to the tangent $\mathbf{t}^{(i)}$ of the current incremental load-displacement configuration. The scalar product of these two vectors yields a residual $R^{(i)}$. Specification of the desired residual defines the direction of the update. Arc length procedures previously obtained through application of specific prerequisite constraint equations can be incorporated into a family of orthogonal plane methods. Normal and updated normal plane [17], consistently linearized spherical hyperplane [20], and explicit spherical [5] iteration procedures can all be derived from this general method.

The tangential and normal vectors exist in a multi-dimensional space. This consists of m dimensions from the displacement vector and 1 dimension from the load parameter. These components are combined using a scaling factor β (with units of displacement) to form vectors with m +1 dimensions.

$$\mathbf{t}^{(i)} = \mathbf{u}^{(i)} + \beta \lambda^{(i)} \tag{2.9}$$

$$\mathbf{n}^{(i)} = \Delta\mathbf{u} + \beta \Delta\lambda \tag{2.10}$$

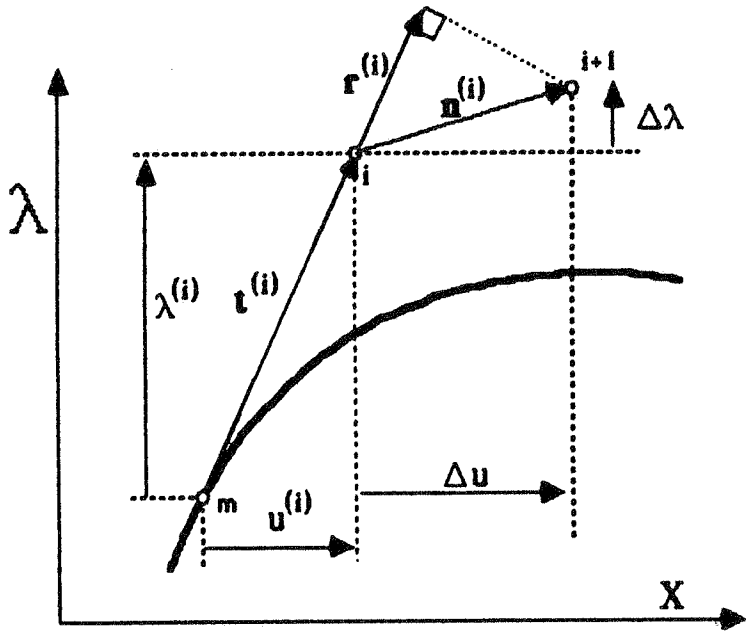

Figure 2.3 Orthogonality Relationship.

The scalar product of these vectors yields a residual $R^{(i)}$. This can be visualized as the projection of vector $\mathbf{n}^{(i)}$ onto vector $\mathbf{t}^{(i)}$ (the length of vector $\mathbf{r}^{(i)}$ multiplied by the length of vector $\mathbf{t}^{(i)}$).

$$\begin{aligned} \mathbf{t}^{(i)} \cdot \mathbf{n}^{(i)} &= |\mathbf{t}^{(i)}|\,|\mathbf{n}^{(i)}| \cos \propto \\ &= |\mathbf{t}^{(i)}|\,|\mathbf{r}^{(i)}| \\ &= R^{(i)} \end{aligned} \tag{2.11}$$

Forming the scalar product of $\mathbf{t}^{(i)}$ and $\mathbf{n}^{(i)}$ using equations 2.6, 2.9, and 2.10, a general expression can be derived for $\Delta\lambda$.

$$\begin{aligned} \mathbf{t}^{(i)} \cdot \mathbf{n}^{(i)} &= \mathbf{u}^{(i)T}\Delta\mathbf{u} + \beta^2\lambda^{(i)}\Delta\lambda \\ &= \mathbf{u}^{(i)T}(\Delta\mathbf{u}^{I}\Delta\lambda + \Delta\mathbf{u}^{II}) + \beta^2\lambda^{(i)}\Delta\lambda \\ &= \mathbf{u}^{(i)T}\Delta\mathbf{u}^{II} + \Delta\lambda(\mathbf{u}^{(i)T}\Delta\mathbf{u}^{I} + \beta^2\lambda^{(i)}) \end{aligned}$$

General Expression (2.12)

$$\Delta\lambda = \frac{R^{(i)} - \mathbf{u}^{(i)T}\Delta\mathbf{u}^{II}}{\beta^2\lambda^{(i)} + \mathbf{u}^{(i)T}\Delta\mathbf{u}^{I}}$$

This expression can be simplified for particular cases of orthogonality. For the case of $R^{(i)} \equiv 0$, the update direction is normal to the tangent vector. If the tangent vector is used from the original configuration then the expression for normal planes is obtained [17].

Normal Planes (2.13)

$$\Delta\lambda = \frac{-\mathbf{u}^{(1)T}\Delta\mathbf{u}^{II}}{\beta^2\lambda^{(1)} + \mathbf{u}^{(1)T}\Delta\mathbf{u}^{I}}$$

If the tangent vector is updated for each equilibrium iteration then the expression for updated normal planes is obtained [17].

Updated Normal Planes (2.14)

$$\Delta\lambda = \frac{- \mathbf{u}^{(i)T}\Delta\mathbf{u}^{II}}{\beta^2\lambda^{(i)} + \mathbf{u}^{(i)T}\Delta\mathbf{u}^{I}}$$

The update direction provided by the normal plane method is always orthogonal to the original tangent. In contrast, the updated normal plane method provides a diverging spiral path tending towards the desired arc.

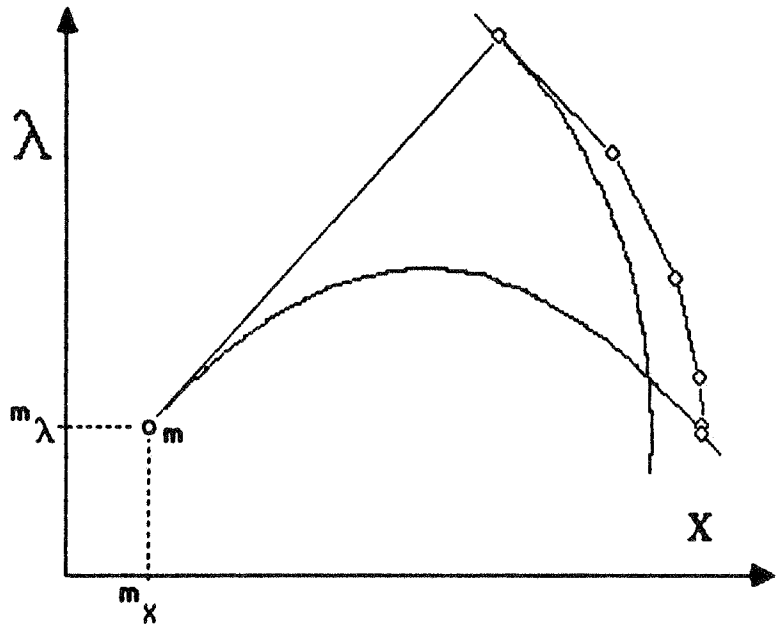

Figure 2.4 Updated Normal Plane Method.

The divergent behaviour of the previous two methods is usually not too important except under extreme conditions encountered near limit points. If further restriction is required for the path then additional orthogonality relations must be investigated.

A simple correction can be applied to the residual once divergence from the arc has taken place. The difference between the length of the current tangent vector and the desired length can be projected onto the current tangent vector to provide the residual for the orthogonality expression.

$$\begin{aligned} t^{(i)} \cdot r^{(i)} &= -|\, t^{(i)}|\, |\, r^{(i)}| \\ &= -t^{(i)}(t^{(i)} - s\,) \\ &= R^{(i)} \end{aligned} \qquad (2.15)$$

Substitution of this residual into the general expression yields an update for linearized iteration on spherical hyperplanes as obtained by [20].

Consistently Linearized (2.16)

$$\Delta\lambda = \frac{-t^{(i)}(t^{(i)} - s) - u^{(i)T}\Delta u^{II}}{\beta^2\lambda^{(i)} + u^{(i)T}\Delta u^{I}}$$

The update direction provided by this method also tends initially away from the arc; however, the application of the residual draws the path back to the circle once convergence is achieved.

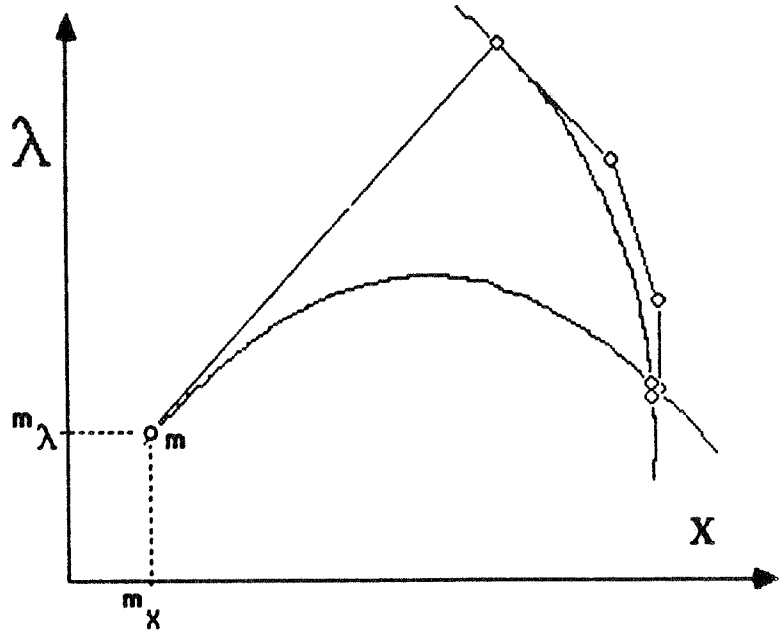

Figure 2.5 Consistently Linearized Method.

Explicit iteration in a circular path requires the formulation of a residual based on the error that would be obtained using an orthogonal iteration path. This error can be corrected in advance to provide the desired arc. The residual vector $r^{(i+1)}$ is in line with the tangent $t^{(i+1)}$ and acts in the opposite direction. The error obtained in iteration i+1 is the difference between the length of the tangent in this configuration and the desired length.

$$|r^{(i+1)}| = |t^{(i+1)}| - |t^{(i)}|$$

$$= (t^{(i+1)} - s) \qquad (2.17)$$

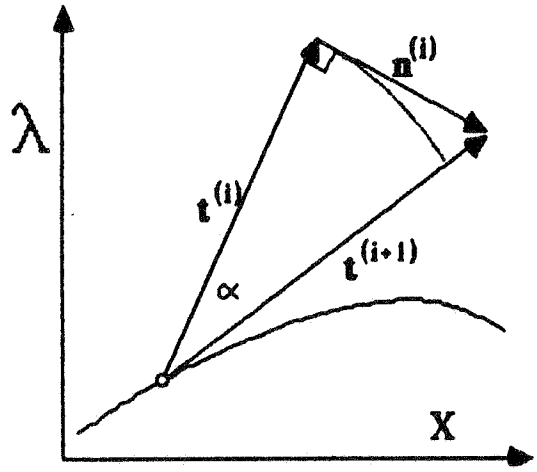

Figure 2.6 Tangent Vectors for Orthogonal Iteration.

The orthogonality condition used to derive the general expression can be applied to the residual vector to provide the scalar residual $R^{(i)}$.

$$t^{(i)} \cdot r^{(i+1)} = -|t^{(i)}||r^{(i+1)}| \cos \alpha$$

$$= -s\,(t^{(i+1)} - s)\frac{s}{t^{(i+1)}}$$

$$= -\frac{s^2}{t^{(i+1)}}(t^{(i+1)} - s)$$

$$= R^{(i)} \qquad (2.18)$$

The length of $t^{(i+1)}$ can be calculated in terms of the old length and the incremental update vector.

$$t^{(i+1)} = \left(t^{(i)2} + \Delta \mathbf{u}^T \Delta \mathbf{u} + \beta^2 \Delta\lambda^2 \right)^{0.5} \tag{2.19}$$

Substitution of this expression into the general formula for $\Delta\lambda$ leads directly to the quadratic equation obtained by Crisfield [5]. The problems encountered in the application of Crisfield's method can be avoided by solving for $t^{(i+1)}$ using the updated normal plane expression for $\Delta\lambda$, and then calculating a residual which returns the iteration direction to a point directly on the sphere (An algorithm is given for this procedure on page 20). This provides the same result as in [5], but does <u>not</u> require the solution of a quadratic equation and the selection of one root.

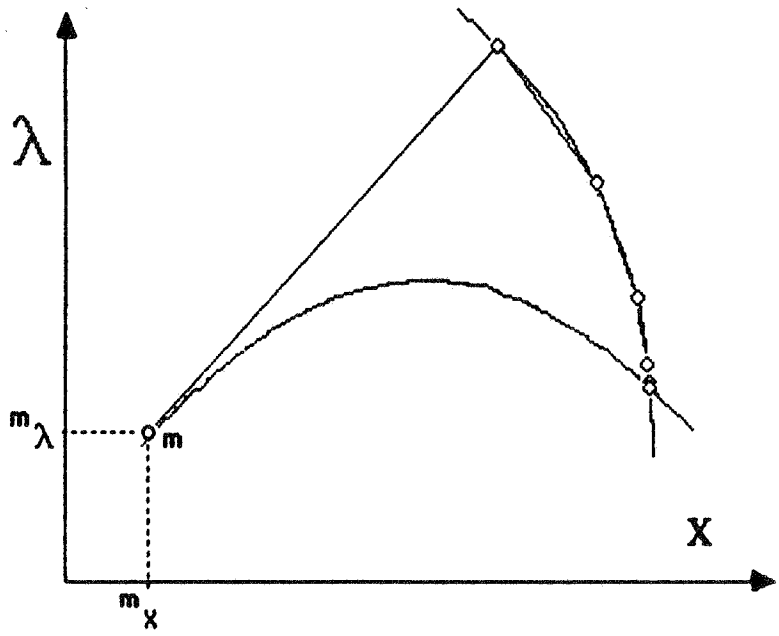

Figure 2.7 Explicit Iteration on Spheres.

Algorithm for Explicit Iteration on Spheres

1. Use the update for orthogonal iteration.

$$\Delta\lambda = \frac{- \mathbf{u}^{(i)T}\Delta\mathbf{u}^{II}}{\beta^2\lambda^{(i)} + \mathbf{u}^{(i)T}\Delta\mathbf{u}^{I}}$$

2. Calculate the associated displacement vector.

$$\Delta\mathbf{u} = \Delta\mathbf{u}^{I}\Delta\lambda + \Delta\mathbf{u}^{II}$$

3. Find the length of the tangent in the potential configuration.

$$t^{(i+1)} = \left(t^{(i)2} + \Delta\mathbf{u}^{T}\Delta\mathbf{u} + \beta^2\Delta\lambda^2 \right)^{0.5}$$

4. Calculate the required residual for explicit iteration on a sphere.

$$R^{(i)} = -\frac{s^2}{t^{(i+1)}}(t^{(i+1)} - s)$$

5. Return to the general formula for iteration path direction.

$$\Delta\lambda = \frac{R^{(i)} - \mathbf{u}^{(i)T}\Delta\mathbf{u}^{II}}{\beta^2\lambda^{(i)} + \mathbf{u}^{(i)T}\Delta\mathbf{u}^{I}}$$

6. Calculate the desired displacement vector.

$$\Delta\mathbf{u} = \Delta\mathbf{u}^{I}\Delta\lambda + \Delta\mathbf{u}^{II}$$

This procedure involves only a small amount of extra work in comparison to that of the consistently linearized procedure. Steps 1, 2, 3, 4, and 5 require the identical amount of computation. Step 6 introduces one additional vector mutiplication and addition. The larger domain of attraction offered by this algorithm, in comparison to the other methods based on orthogonality, may be important in the vicinity of limit points with sharp gradients.

2.1.2 Consistently Linearized Method

The results previously derived using orthogonality principles can also be derived by the consistent linearization of a general path following scheme. This involves the introduction of an arbitrary constraint equation to the system of equilibrium equations and the subsequent reduction to a set of equations of original size. This reduction is done via elimination of $\Delta\lambda$ as given by Schweizerhof and Wriggers [20].

2.1.3 Crisfield's Method

Iteration on spheres can be performed by the introduction of a constraint equation which is explicitly satisfied at every equilibrium iteration. The approach of Crisfield [5] can be derived starting from the definition of the current and following load/displacement configurations.

$$t^{(i)2} = \beta^2\lambda^{(i)2} + \mathbf{u}^{(i)T}\mathbf{u}^{(i)} \tag{2.20}$$

$$t^{(i+1)2} = \beta^2(\lambda^{(i)}+\Delta\lambda)^2 + (\mathbf{u}^{(i)}+\Delta\mathbf{u}^{I}\Delta\lambda+\Delta\mathbf{u}^{II})^T(\mathbf{u}^{(i)}+\Delta\mathbf{u}^{I}\Delta\lambda+\Delta\mathbf{u}^{II}) \tag{2.21}$$

The solution employed by Crisfield in [5] utilizes a further simplification of β=0 at this stage; however, this is included here for consistency of the derivation. The two configurations $t^{(i)}$ and $t^{(i+1)}$ are identically equal to the prescribed value of the arc length. Combination of the two expressions yields a quadratic equation.

$$a\Delta\lambda^2 + b\Delta\lambda + c = 0 \tag{2.22}$$

where:

$$a = \beta^2+\Delta\mathbf{u}^{I^T}\Delta\mathbf{u}^{I}$$

$$b = 2(\beta^2\lambda^{(i)}+\mathbf{u}^{(i)^T}\Delta\mathbf{u}^{I}+\Delta\mathbf{u}^{II^T}\Delta\mathbf{u}^{I})$$

$$c = 2\mathbf{u}^{(i)^T}\Delta\mathbf{u}^{II}+\Delta\mathbf{u}^{II^T}\Delta\mathbf{u}^{II}$$

The solution yields two roots for $\Delta\lambda$:

$$\Delta\lambda = \frac{-b \pm \sqrt{b^2 - 4ac}}{2a}$$

The selection of the appropriate root depends on the current tendency of the load/displacement curve. Precautions must also be taken in the case of complex roots. The solutions of these problems are explained by Crisfield [5].

2.1.4 Theoretical Comparison of the Methods

The performance of arc length procedures depends on the nature of the load/displacement response curve. A typical problem found in shell analysis is geometric snap-through. A sine wave is characteristic of problems involving repetitious loading/unloading. Using a common arc length and convergence criteria, a theoretical comparison can be made between the various methods. The stability, convergence rate, and numerical efficiency of the methods are compared here for a variety of iteration conditions.

Given a load/displacement curve following the relation 2.23, it is possible to explicitly calculate the stiffness expression for a one dimensional problem.

$$\lambda = 2 \sin x \tag{2.23}$$

All previously mentioned methods were tested using a simple spreadsheet program. Initially the arc length was fixed at a unit length and the convergence was determined when the unbalanced forces numerically approached zero ($G^{(i)} < 10^{-4}$). This analysis provided the iteration paths given in figures 2.8 to 2.12.

Normal Plane Iteration

The potential divergent behaviour of this method is shown in figure 2.8.

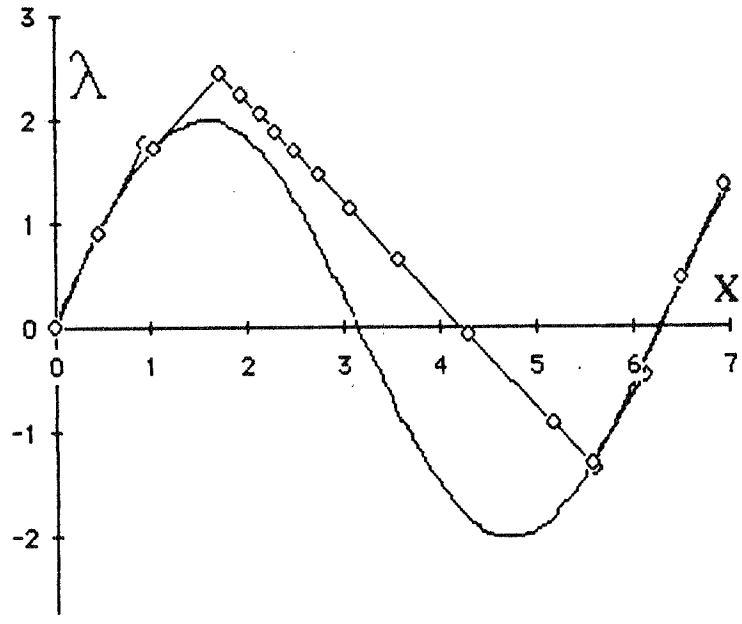

Figure 2.8 Normal Plane Iteration.

Updated Normal Plane Iteration

The updated nomal plane formula intially demonstrated the same divergent characteristic, however convergence was obtained once more via a divergent spiral path. This effect was magnified in the vicinity of the limit points.

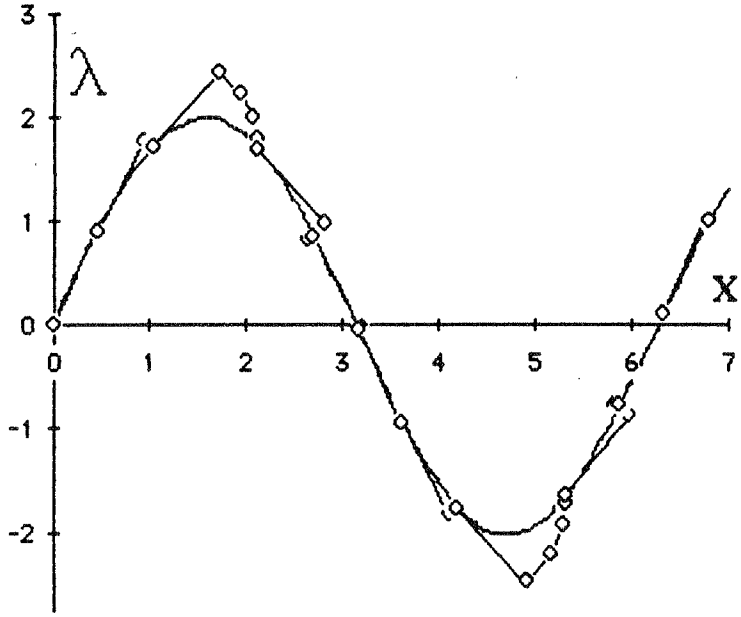

Figure 2.9 Updated Normal Plane Iteration.

Explicit Iteration on Spheres

This method leads to a consistent incremental progression along the path given by a prescribed arc length. Iteration appears to be more stable than the preceeding methods.

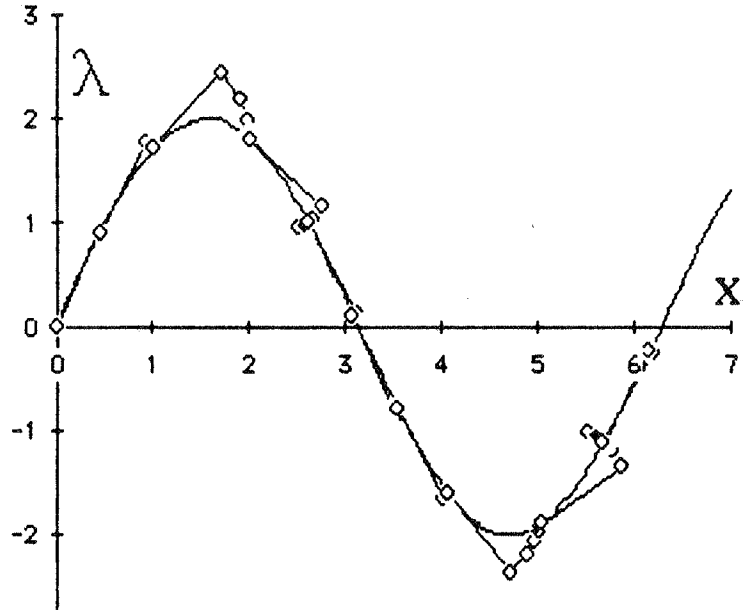

Figure 2.10 Iteration on Spheres using Orthogonality.

Consistently Linearized Iteration

Iteration on spherical hyperplanes, provided by the consistently linearized method [20], had substantially the same behaviour as explicit iteration on spheres for this problem. The domain of attraction is only slightly smaller for this method so differences would only be expected in extreme cases.

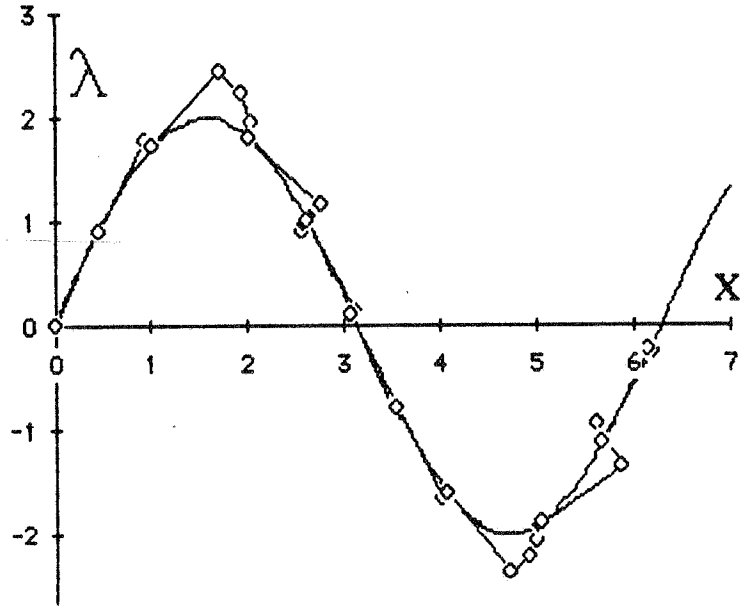

Figure 2.11 Consistently Linearized Iteration.

Explicit Iteration on Spheres

Crisfield's method provided the same results as found for explicit iteration on spheres using orthogonality.

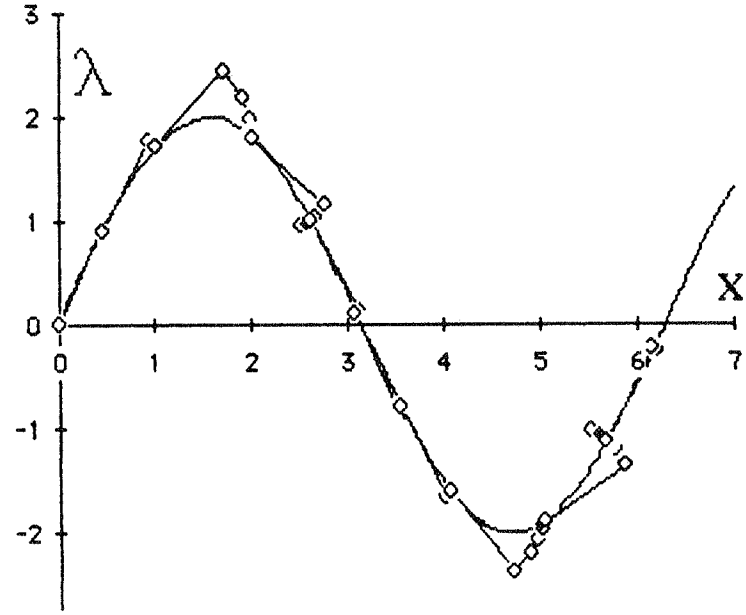

Figure 2.12 Crisfield's Method.

To investigate the performance of the various methods in the vicinity of a limit point, the second arc length step (m=2) was chosen. Up to this point, convergence was essentially identical for all methods.

A plot of the unbalanced forces $G^{(i)}$ throughout the equilibrium iteration process reveals the differences in the convergence behaviour of the individual schemes. Normal plane iteration diverges from the sine wave (as seen in figure 2.8) and only converges by chance again at another point further down the curve. The other methods all converge with relatively no problem. As predicted, explicit iteration on spheres provides the identical result as found using Crisfield's method (with some small numerical discrepancy). The updated normal plane and the consistently linearized methods start in the same direction, however once deviation occurs from the explicit iteration path a residual appears in the update for the linearized method. This residual draws the following iteration towards the spherical path and stabilizes the iteration. A pattern of continuously linearized updates is followed until convergence is ultimately obtained at the same point as that defined by explicit iteration on spheres.

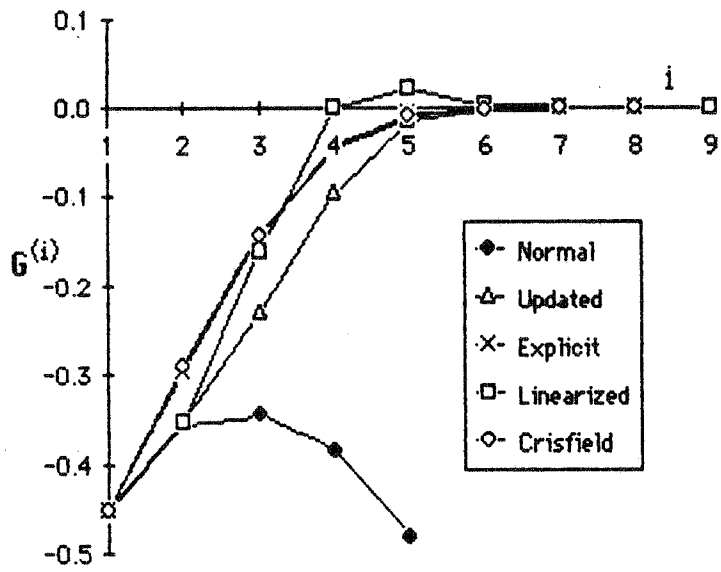

Figure 2.13 Convergence of the Unbalanced Forces.

The general tendencies of the methods can be demonstrated easily by looking at the convergence velocity. The normal plane method again has divergency demonstrated by the initial behaviour in comparison to the other procedures. The initial velocities of the normal, updated normal, and linearized methods are identical. The linearized procedure follows the example of explicit iteration on spheres with some lag factor.

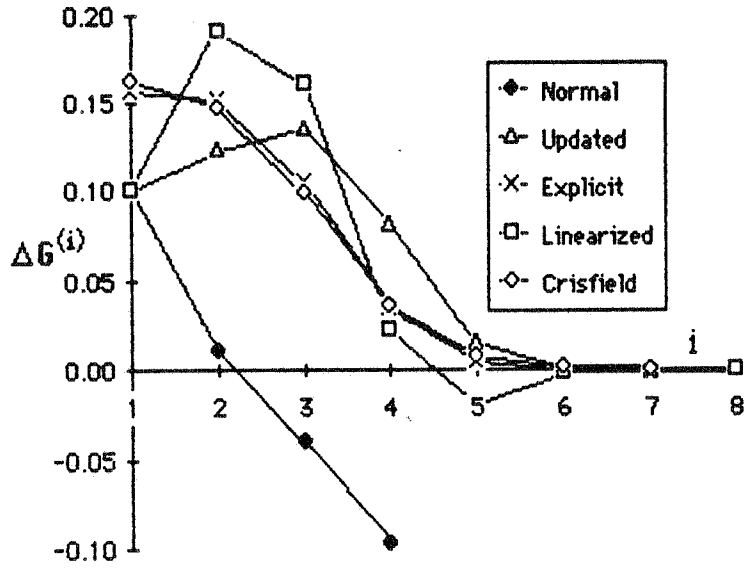

Figure 2.14 Convergence Velocity.

No realistic distinction in the rate of convergence can be singly based on one iteration group. A general tendency was found from the average of nine tests which indicates that all of the methods appear to converge at approximately the same rate for a given arc length, and that the number of iterations required is dependent on the length of the step. The primary distinction between the methods appears in extreme conditions of nonlinearity where the simple methods fail to converge. The application of pure Newton updates to the stiffness improved the convergence rates and general behaviour of all methods.

Numerical divergence may occur when arc length procedures are used in conjunction with Newton iteration schemes. The problem arises from the potential alignment of the update vector and the tangent stiffness under extremely nonlinear conditions. If these two vectors are approximately parallel then the calculation of an update produces an error which can be much larger than the original unbalanced forces. This can cause complete divergence for all orthogonality methods as well as local divergence for Crisfield's method. This effect is evident in the path followed by the explicit iteration on spheres using orthogonality (Figure 2.15). Using the slope at the start of the arc length step (modified Newton), it is not possible to trace the path past the tangent of this slope on the other side of the sphere.

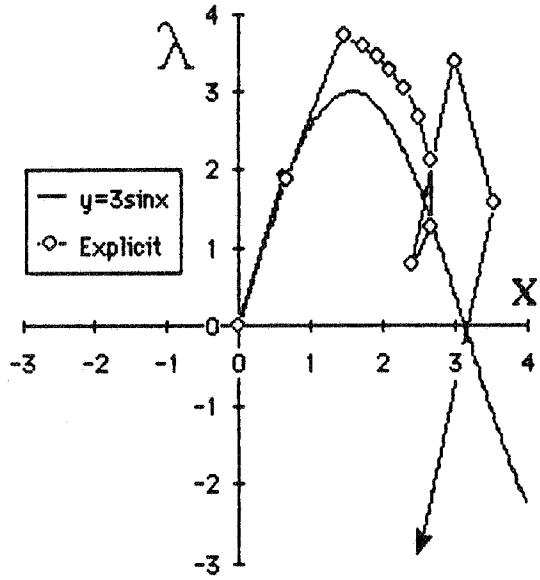

Figure 2.15 Divergence of Explicit Iteration on Spheres.

The same problem occurs with Crisfield's method. Once this kind of critical point is reached, iteration must be completely terminated since the roots of the quadratic expression for $\Delta\lambda$ become imaginary. This indicates that the failure of Crisfield's method is caused by the same geometric problem associated with the failure of explicit iteration on spheres based on orthogonality.

A second type of divergence can occur when using orthogonality procedures with the pure Newton method. If the stiffness radically changes direction between increments then a false update may occur. This is analogous with choosing the wrong root from Crisfield's method. A simple check can be included in the updating procedure to choose the alternative direction if such a change in stiffness has occured. Using quasi Newton methods may also avoid this problem since the secant stiffness will be less likely to radically change direction between increments.

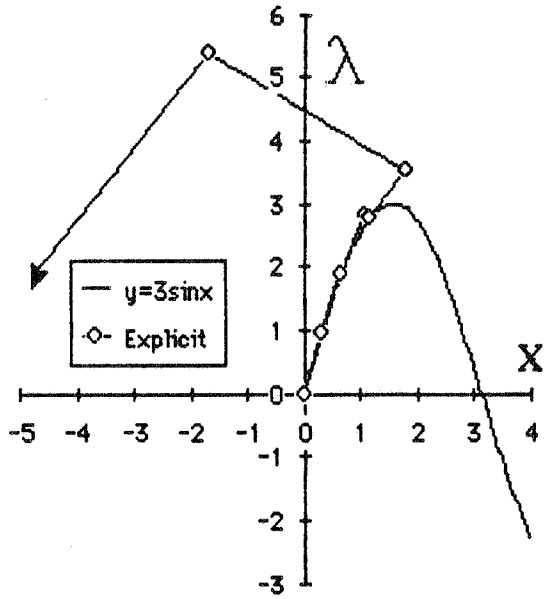

Figure 2.16 False Update Divergence.

A summary of the preceeding analysis is given in appendix A.

2.2 Quasi Newton Methods

Providing updates for the stiffness matrix using a simple correction at every equilibrium step, rather than recomputing it entirely (pure Newton) or leaving it unaltered (modified Newton), is the foundation for quasi Newton methods. Matrix update formulae are extensively documented in recent literature. A summary is given here to clarify their application in conjunction with the arc length procedures used in the present numerical studies.

Construction of a secant matrix for incremental iteration can be obtained via several different formulations. The general quasi Newton equations for use with arc length procedures stem from linearization of the variation between successive equilibrium iterations.

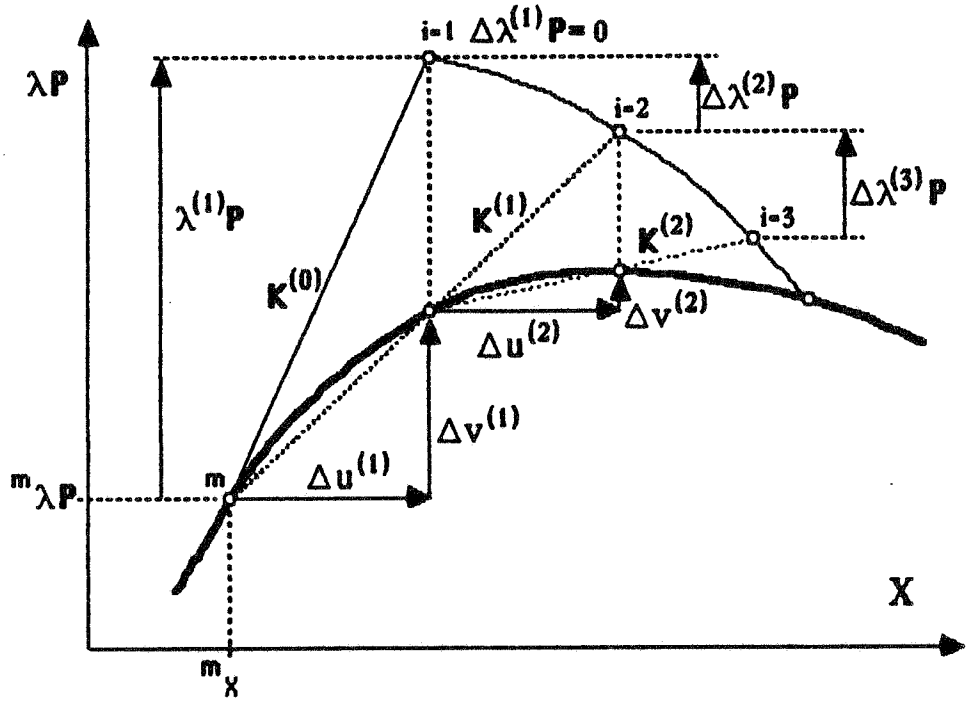

Figure 2.17 Quasi Newton Updates for $K^{(i)}$.

A set of quasi Newton equations can be derived for arbitrary Δu and $\Delta\lambda$.

$$K^{(i)}\Delta u^{(i)} = (\lambda^{(i)}-\lambda^{(i-1)})\,P - (F^{(i)}- F^{(i-1)}) + \Delta\lambda^{(i)}\,P \qquad (2.24)$$

This expression can also be written in terms of the difference between the total out of balance load vector v in successive iterations.

$$\begin{aligned} K^{(i)}\Delta u^{(i)} &= (^{m}\lambda+\lambda^{(i)})\,P - (^{m}\lambda+\lambda^{(i-1)})\,P - (F^{(i)}- F^{(i-1)}) + \Delta\lambda^{(i)}\,P \\ &= ((^{m}\lambda+\lambda^{(i)})\,P - F^{(i)}) - ((^{m}\lambda+\lambda^{(i-1)})\,P - F^{(i-1)}) + \Delta\lambda^{(i)}\,P \\ &= v^{(i)}- v^{(i-1)} + \Delta\lambda^{(i)}\,P \\ &= \Delta v^{(i)} + \Delta\lambda^{(i)}\,P \end{aligned} \qquad (2.25)$$

2.2.1 Rank One Updates

Satisfaction of the quasi Newton equations (2.25) can be achieved via many different formulations. Most common methods utilize one of two classes of updates. The first involves the generation of an update using one correction term (rank one), while the second uses two correction terms (rank two). The update from Broyden provides a close approximation to K, however the resulting matrices are nonsymmetrical. This is not a problem if the inverse is directly updated in vector form (2.26). This kind of update requires storage of 2 vectors and 1 factor per iteration.

Broyden

$$\mathbf{K}^{(i)^{-1}} = \mathbf{K}^{(i-1)^{-1}} + \alpha^{(i)}\, \mathbf{w}^{(i)} \Delta \mathbf{u}^{(i)^T}\, \mathbf{K}^{(i-1)^{-1}} \tag{2.26}$$

$$\mathbf{w}^{(i)} = \Delta \mathbf{u}^{(i)} - \mathbf{K}^{(i-1)^{-1}} (\Delta \mathbf{v}^{(i)} + \Delta \lambda^{(i)}\, \mathbf{p}) \tag{2.27}$$

$$\alpha^{(i)} = \frac{1}{\Delta \mathbf{u}^{(i)^T} (\Delta \mathbf{u}^{(i)} - \mathbf{w}^{(i)})} \tag{2.28}$$

The update from Davidon provides a symmetrical approximation to the inverse of K which can again be directly updated in vector form (2.29). This kind of update requires storage of only 1 vector and 1 factor per iteration.

Davidon

$$\mathbf{K}^{(i)^{-1}} = \mathbf{K}^{(i-1)^{-1}} + \alpha^{(i)}\, \mathbf{w}^{(i)}\, \mathbf{w}^{(i)^T} \tag{2.29}$$

$$\mathbf{w}^{(i)} = \Delta \mathbf{u}^{(i)} - \mathbf{K}^{(i-1)^{-1}} (\Delta \mathbf{v}^{(i)} + \Delta \lambda^{(i)}\, \mathbf{p}) \tag{2.30}$$

$$\alpha^{(i)} = \frac{1}{\mathbf{w}^{(i)^T} (\Delta \mathbf{v}^{(i)} + \Delta \lambda^{(i)}\, \mathbf{p})} \tag{2.31}$$

2.2.2 Rank Two Updates

Generation of updates using two correction terms provides many potential forms. The Davidon [6], Fletcher/Powell [7] update (DFP) provides a stiffness matrix built from two symmetrical components. This formulation requires the storage of 2 vectors and 2 factors per iteration for the vector form (2.32).

DFP

$$\mathbf{K}^{(i)^{-1}} = \mathbf{K}^{(i-1)^{-1}} + \alpha^{(i)}\,\Delta\mathbf{u}^{(i)}\Delta\mathbf{u}^{(i)^T} - \beta^{(i)}\,\mathbf{w}^{(i)}\,\mathbf{w}^{(i)^T} \tag{2.32}$$

$$\mathbf{w}^{(i)} = \mathbf{K}^{(i-1)^{-1}}(\Delta\mathbf{v}^{(i)} + \Delta\lambda^{(i)}\,\mathbf{P}) \tag{2.33}$$

$$\alpha^{(i)} = \frac{1}{\Delta\mathbf{u}^{(i)^T}(\Delta\mathbf{v}^{(i)} + \Delta\lambda^{(i)}\,\mathbf{P})} \tag{2.34}$$

$$\beta^{(i)} = \frac{1}{\mathbf{w}^{(i)^T}(\Delta\mathbf{v}^{(i)} + \Delta\lambda^{(i)}\,\mathbf{P})} \tag{2.35}$$

The most popular rank 2 updates are derived from the BFGS (Broyden [2], Fletcher [8], Goldfarb [10], Shanno [22]) formulation. Two forms for use with arc length procedures have been provided by Matthies/Strang [13] and a third was developed specially for use with arc length procedures by Schweizerhof/Wriggers [20]. The general update can be written in vector form requiring the storage of 2 vectors and 2 factors per iteration (2.36).

BFGS

$$\mathbf{K}^{(i)^{-1}} = \mathbf{K}^{(i-1)^{-1}} - \alpha^{(i)}\,(\Delta\mathbf{u}^{(i)}\mathbf{w}^{(i)^T} + \mathbf{w}^{(i)}\Delta\mathbf{u}^{(i)^T}) - \beta^{(i)}\Delta\mathbf{u}^{(i)}\Delta\mathbf{u}^{(i)^T} \tag{2.36}$$

$$\mathbf{w}^{(i)} = \mathbf{K}^{(i-1)^{-1}}(\Delta\mathbf{v}^{(i)} + \Delta\lambda^{(i)}\,\mathbf{P}) \tag{2.37}$$

$$\alpha^{(i)} = \frac{1}{\Delta\mathbf{u}^{(i)^T}(\Delta\mathbf{v}^{(i)} + \Delta\lambda^{(i)}\,\mathbf{P})} \tag{2.38}$$

$$\beta^{(i)} = \alpha^{(i)}\,(\,\alpha^{(i)}\,\mathbf{w}^{(i)^T}(\Delta\mathbf{v}^{(i)} + \Delta\lambda^{(i)}\,\mathbf{P}) + 1\,) \tag{2.39}$$

3. A Truss Finite Element for Nonlinear Analysis

Ultimate load analysis of space truss structures requires representation of the elastic, plastic, and buckling phenomena found under large displacement conditions. The BTRUSS finite element was developed specifically for this purpose, and is documented in the following. Newton iteration schemes, used for the solution of nonlinear equilibrium equations, require the tangent stiffness. Kinematic, geometric, constitutive, and equilibrium relations are used to derive the stiffness of a truss for elastic, plastic, and post-buckling behaviour. Bifurcation member buckling is modelled using an approximate solution for the elastic problem as proposed by Kondoh and Atluri [12].

3.1 Kinematics

The truss is one of the simplest elements available for structural analysis. In elementary statics, truss elements are often called "two force members" since there are only two forces that act on a truss in equilibrium. The nodal reactions are equal, and act opposingly in line with the truss. Stresses exist in only one direction, so by application of kinematics this can be reduced to a one dimensional problem. An investigation into the behaviour of a three dimensional body leads to this formulation.

Solution of a general continuum mechanics problem requires the selection of a reference state. The Euler (Cauchy) formulation uses the deformed configuration, while the Lagrange formulation uses the initial (undeformed) configuration. The obvious advantage of the Lagrange formulation is the natural reference to the initial known state. Strains computed using the Green-Lagrange tensor refer to fibers originally in line with the coordinate axes although they are now in a deformed position. This means that rigid body modes are contained within the strain definition. The Kirchhoff-Piola pseudo stress tensor (KP2) is obtained by applying two deformation gradient transformations to the Cauchy stress tensor. This effectively aligns the stress tensor to the deformed configuration although reference is still to the original geometry. The combination of the Green-Lagrange strain and the Kirchhoff-Piola (KP2) pseudo stress is widely used for the solution of nonlinear continuum mechanics problems since this provides the link between the initial known configuration, and the load applied to the deformed body.

For a truss element this problem is vastly simplified. The use of a local moving coordinate system allows the superposition of pure strains on top of the rigid body modes. The traditional engineering approach, which assumes small rotations within single elements, is exact for the truss by definition. Since the deformed configuration is essentially known in a one dimensional problem, reference can be made directly to Cauchy stresses. The truss element is thus most efficiently formulated in one dimension using engineering strains and Cauchy stresses, and then simply transformed to three dimensions for use as a space truss.

3.2 Geometry

Transformations of geometry must be done first for the calculation of global stiffness from local stiffness, and again for the calculation of local displacements resulting from global displacements.

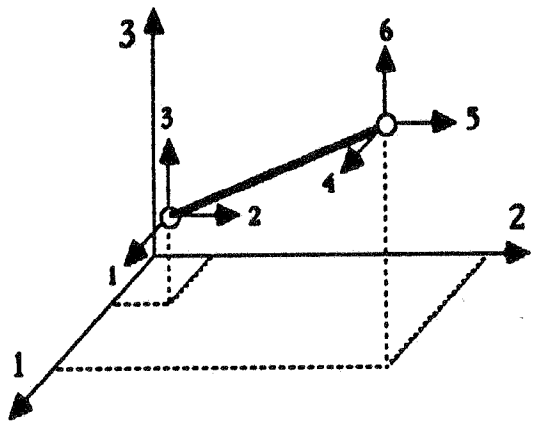

Figure 3.1 BTRUSS Global Configuration.

The axial stiffness of a truss element, with direction cosines (c_1 , c_2 , c_3), can be represented by global stiffness components for each of the six nodal degrees of freedom. The global stiffness matrix for a truss with axial stiffness k in configuration m is transformed by two direction vectors ${}^{m}\mathbf{c}$ whose product yields the direction cosine matrix ${}^{m}\mathbf{C}$ for a truss element.

$$\underset{6x6}{{}^{m}\mathbf{K}} = \underset{6x2}{{}^{m}\mathbf{c}^{T}}\ \underset{2x2}{{}^{m}\mathbf{k}}\ \underset{2x6}{{}^{m}\mathbf{c}} = \underset{6x6}{{}^{m}\mathbf{k}\,{}^{m}\mathbf{C}} \qquad (3.1)$$

This provides a global stiffness in terms of direction cosines in the deformed three dimensional configuration and a parameter k from the one dimensional solution. The complete global stiffness for a single truss element can be written in expanded form using these parameters.

$$
{}^{m}K = k \begin{bmatrix}
c_1c_1 & c_1c_2 & c_1c_3 & -c_1c_1 & -c_1c_2 & -c_1c_3 \\
c_2c_1 & c_2c_2 & c_2c_3 & -c_2c_1 & -c_2c_2 & -c_2c_3 \\
c_3c_1 & c_3c_2 & c_3c_3 & -c_3c_1 & -c_3c_2 & -c_3c_3 \\
-c_1c_1 & -c_1c_2 & -c_1c_3 & c_1c_1 & c_1c_2 & c_1c_3 \\
-c_2c_1 & -c_2c_2 & -c_2c_3 & c_2c_1 & c_2c_2 & c_2c_3 \\
-c_3c_1 & -c_3c_2 & -c_3c_3 & c_3c_1 & c_3c_2 & c_3c_3
\end{bmatrix}
$$

The length in the deformed configuration, calculated from the global displacements, provides the strain condition of figure 3.2. This is used to calculate the stress condition from the material law and then to update the one dimensional stiffness k.

Figure 3.2 BTRUSS Local Configuration.

3.3 Constitutive Expression

The state of a truss element can be completely described in the deformed configuration by the length ${}^{m}L$, the cross sectional area ${}^{m}A$, and the applied axial stress ${}^{m}\sigma$. These parameters can be related to the initial geometry and the current load condition through the constitutive equations derived from the strain and material laws.

The axial strain for a one dimensional truss can be written using a linear expression in terms of the deformed and original lengths.

$$
{}^{m}\epsilon = \frac{{}^{m}L - {}^{0}L}{{}^{0}L} = \frac{{}^{m}x}{{}^{0}L} \tag{3.2}
$$

Using the preceeding engineering strain definition, the strain increment can be written in terms of the displacement increment.

$$
\epsilon = {}^{2}\epsilon - {}^{1}\epsilon = \frac{u}{{}^{0}L} \tag{3.3}
$$

Stresses are applied to a truss in only one direction; however, strains exist in all three dimensions. The traditional engineering approach for truss problems is to assume that ${}^{m}A$ is constant (strains exist only in the axial direction). This is only valid for small strains.

A better result can be obtained by including the effect of strains in the other directions through the application of Poisson's ratio. The specific approximation required for a truss element is the relation between the reduced area and the area in the undeformed configuration. This relationship is material dependent. The engineering stress definition assumes an unaltering cross sectional area. This provides the exact result for materials with $\upsilon = 0$. Another common definition is for the volume to remain constant through deformation (good for materials with $\upsilon = 0.5$). A general expression with υ as a parameter is derived here and then later a value which is applicable for steel ($\upsilon = 0.3$) is used in BTRUSS.

Poisson's ratio provides the relationship between axial and lateral strains. This can be used to express the deformed cross sectional area of a truss member in terms of the axial strain condition.

$$ {}^{m}A = {}^{0}A\,(1 - {}^{m}\epsilon\upsilon)^2 \qquad (3.4) $$

Incrementation of this expression provides the area in the deformed configuration in terms of the original area, the current strain condition, and the awaited strain increment.

$$
\begin{aligned}
{}^{2}A &= {}^{0}A(1-{}^{2}\epsilon\upsilon)^2 \\
&= {}^{0}A(1-({}^{1}\epsilon+\epsilon)\upsilon)^2 \\
&= {}^{0}A(1-2({}^{1}\epsilon+\epsilon)\upsilon+({}^{1}\epsilon+\epsilon)^2\upsilon^2) \\
&= {}^{0}A(1-2({}^{1}\epsilon+\epsilon)\upsilon+({}^{1}\epsilon^2+2{}^{1}\epsilon\epsilon+\epsilon^2)\upsilon^2) \\
&= {}^{0}A((1-2{}^{1}\epsilon\upsilon+{}^{1}\epsilon^2\upsilon^2)+(-2\epsilon\upsilon+2{}^{1}\epsilon\epsilon\upsilon^2+\epsilon^2\upsilon^2)) \\
&= {}^{0}A((1-{}^{1}\epsilon\upsilon)^2-2\epsilon\upsilon(1-{}^{1}\epsilon\upsilon)+\epsilon^2\upsilon^2) \\
&= {}^{0}A(1-{}^{1}\epsilon\upsilon)^2\{1-2\epsilon\upsilon(1-{}^{1}\epsilon\upsilon)^{-1}+\epsilon^2\upsilon^2(1-{}^{1}\epsilon\upsilon)^{-2}\} \qquad (3.5)
\end{aligned}
$$

3.4 Equilibrium

The stress can also be written in incremental form.

$$^2\sigma = {}^1\sigma + \sigma \tag{3.6}$$

Combination of the stress increment and the constitutive expression yields the incremental axial force in terms of $\epsilon(u)$ and $\sigma(u)$. Linearization allows the construction of a tangent stiffness for use in a Newton iteration procedure.

$$\begin{aligned} {}^2S &= {}^2\sigma\, {}^2A \\ &= ({}^1\sigma + \sigma)\, {}^0A(1-{}^1\epsilon\upsilon)^2\{1 - 2\epsilon\upsilon(1-{}^1\epsilon\upsilon)^{-1} + \epsilon^2\upsilon^2(1-{}^1\epsilon\upsilon)^{-2}\} \\ &\approx {}^1\sigma\, {}^0A(1-{}^1\epsilon\upsilon)^2\{1 - 2\epsilon\upsilon(1-{}^1\epsilon\upsilon)^{-1} + \ldots\} + \sigma\, {}^0A(1-{}^1\epsilon\upsilon)^2\{1 + \ldots\} \\ &\approx {}^1S - {}^1S(2\epsilon\upsilon)(1-{}^1\epsilon\upsilon)^{-1} + \sigma\, {}^0A(1-{}^1\epsilon\upsilon)^2 \end{aligned} \tag{3.7}$$

3.5 Elastic Stiffness

The incremental elastic stress comes from Hooke's law.

$$\sigma = E\epsilon \tag{3.8}$$

In common notation, this yields the incremental elastic stiffness equation.

$$\begin{aligned} \lambda P - F(x) &\approx - {}^1S(2\upsilon\epsilon)(1-{}^1\epsilon\upsilon)^{-1} + E^0A\epsilon(1-{}^1\epsilon\upsilon)^2 \\ &\approx - \frac{{}^1S}{{}^0L}\frac{2\upsilon}{(1-{}^1\epsilon\upsilon)} \cdot u + \frac{E^0A}{{}^0L}(1-{}^1\epsilon\upsilon)^2 \cdot u \end{aligned} \tag{3.9}$$

In the case where $\upsilon = 0$, the first term drops out and the second term reduces to the linear stiffness. This is the same result as derived using engineering relations where the area is assumed constant throughout deformation. For $\upsilon = 0.5$, this expression reduces to approximately the same result as obtained from a derivation where the volume is assumed to remain constant. In general, for $\upsilon > 0$, the stiffness is reduced by positive axial strain and by the associated axial load.

3.6 Plastic Stiffness

A material law which includes plastic yielding can be easily applied to the truss element. Strain hardening effects have been included in BTRUSS. The model requires an elastic modulus, yield and maximum stresses, as well as a maximum strain (Figure 3.3). From the mentioned parameters, a reduced modulus ^{Y}E (for yielding region) can be calculated and then used in the stiffness expression for the elastic case.

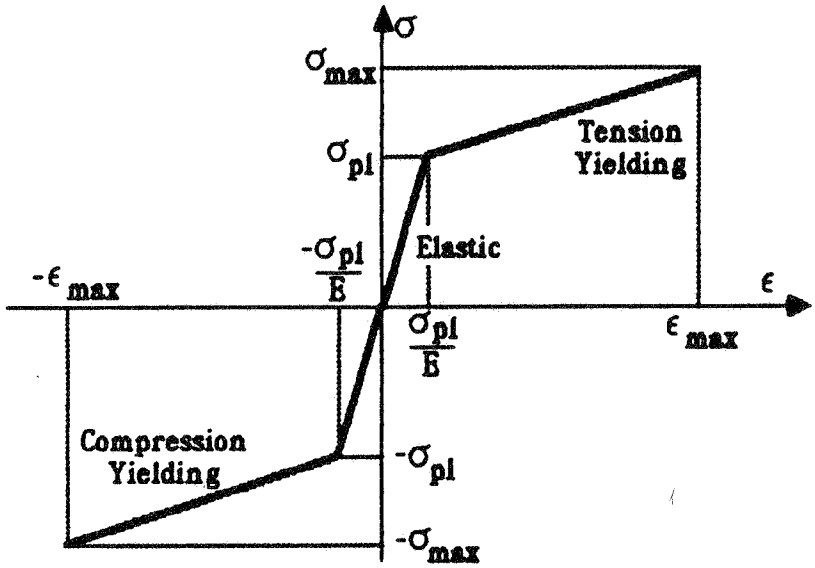

Figure 3.3 BTRUSS Material Law.

The extent of the plastic yielding must be recorded at each step to account for unloading and the return to elastic behaviour. The yielding condition derived here is strictly for constant axial strain over the cross section and does not include bending stresses.

3.7 Post-Buckling Stiffness

A simplified procedure, proposed by Kondoh and Atluri [12], is used for the post-buckling analysis of a truss element. The exact solution for an elastic element has been treated in detail by Timoshenko and Gere [25]. Relations for the axial stretch and the lateral buckling displacement of the element can be written in terms of elliptic integrals. These expressions have been simplified using the first two terms of a series expansion by Byrd and Friedman [3] and later applied by Kondoh and Atluri to an elastic plane truss element. The solution was shown to provide accurate results for axial deformations of up to 15 percent for elastic material.

Derivation of the stiffness matrix in the post-buckling range is somewhat different from the elastic and plastic cases. The nonlinear stress definition, based on the relationship between the axial strain and the cross sectional area, is no longer applicable since the axial strain is not constant once the truss is in the post-buckling configuration. A more useful approximation is the engineering relation (${}^{m}A = {}^{0}A$).

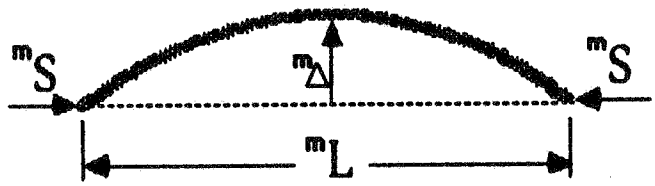

Figure 3.4 Post-Buckling Configuration.

A solution for buckled truss elements has been derived by Kondoh and Atluri which provides the two basic equations applied in the following. The post-buckling load capacity, and the transverse displacement at midspan are written in terms of an effective axial strain ê.

$$ {}^{m}S \approx {}^{E}S\,(1 - 0.5\,{}^{m}\hat{e}) \tag{3.10} $$

$$ {}^{m}\Delta \approx \frac{{}^{0}L}{\pi}\left\{-{}^{m}\hat{e}\,(4 + {}^{m}\hat{e})\right\}^{0.5} \tag{3.11} $$

$$ {}^{m}\hat{e} = \frac{{}^{m}\delta}{{}^{0}L} \tag{3.12} $$

$$ {}^{E}S = -\frac{\pi^2 EI}{{}^{0}L^2} \tag{3.13} $$

Where ${}^{m}\delta$ is the elongation after buckling, and ${}^{E}S$ is the Euler buckling load.

The first expression can be used to obtain the incremental load equation.

$$^{2}S \approx {}^{E}S\,(1 - 0.5\,{}^{2}\hat{e})$$

$$^{1}S \approx {}^{E}S\,(1 - 0.5\,{}^{1}\hat{e})$$

$$^{2}S - {}^{1}S \approx {}^{E}S(-0.5\,(^{2}\hat{e} - {}^{1}\hat{e})) = -0.5\,{}^{E}\underset{0}{\underset{L}{S}}\,u$$

This equation can also be written in common notation to yield the stiffness expression for a buckled member.

$$\lambda P - F(x) \approx -0.5\,{}^{E}\underset{0}{\underset{L}{S}} \cdot u \qquad (3.14)$$

The transverse displacement at midspan ${}^{m}\Delta$ is not necessary for the construction of the tangent stiffness, but it is useful for the determination of the maximum stress in the buckled truss. The expression from Kondoh and Atluri can be simplified for small values of $\hat{e}$.

$$\begin{aligned} {}^{m}\Delta &\approx \frac{L}{\pi}\,\{-{}^{m}\hat{e}\,(4 + {}^{m}\hat{e})\}^{0.5} \\ &\approx \frac{2L}{\pi}\,(-{}^{m}\hat{e})^{0.5} \\ &\approx 0.6366L\,(-{}^{m}\hat{e})^{0.5} \end{aligned} \qquad (3.15)$$

This simplified expression provides results differing only by 0.6 percent from the more exact formula for effective strains of 5 percent.

The maximum stress in the buckled truss is found in the inner fiber at midspan. This can be approximated using engineering beam theory. The bending moment at midspan is simply ${}^{m}S \cdot {}^{m}\Delta$, so the equation for ${}^{m}\Delta$ can be directly applied. The post-buckling axial load comes from the first Kondoh and Atluri formula. Further simplification of the expression comes from the use of the radius of gyration ($I = Ar^2$), an effective slenderness factor ($\eta = 0.6366 \cdot c/r$), the Euler buckling stress (${}^{E}\sigma$), and a factor f.

$$
\begin{aligned}
{}^{m}\sigma &\approx \frac{{}^{m}S}{A} + \frac{Mc}{I} \\
&\approx \frac{{}^{m}S}{A} + \frac{{}^{m}S}{A} \cdot \frac{{}^{m}\Delta \cdot c}{r^2} \\
&\approx \frac{{}^{m}S}{A} + \frac{{}^{m}S}{A} \cdot \frac{0.6366\ c}{r} \cdot \frac{L}{r} \left(-{}^{m}\hat{e}\right)^{0.5} \\
&\approx \frac{{}^{m}S}{A} \left(1 + \eta \cdot \frac{L}{r} \cdot \left(-{}^{m}\hat{e}\right)^{0.5}\right) \\
&\approx \frac{{}^{E}S}{A} \left(1 - 0.5\,{}^{m}\hat{e}\right) \left(1 + \eta \cdot \frac{L}{r} \cdot \left(-{}^{m}\hat{e}\right)^{0.5}\right) \\
&\approx {}^{E}\sigma \cdot f
\end{aligned}
\qquad (3.16)
$$

Introduction of an effective slenderness ratio allows the calculation of the stress amplification factor (f) from the curves given in figure 3.5.

$$
\begin{aligned}
\frac{{}^{eff}L}{r} &= 0.6366 \cdot \frac{c}{r} \cdot \frac{L}{r} \\
&= \eta \cdot \frac{L}{r}
\end{aligned}
\qquad (3.17)
$$

The value of η depends on the particular cross section (For thin walled tubes η =0.91 and for round bars η =1.27). This can be calculated for any cross section given the radius of gyration r and the distance to the outer fiber c.

The amplification factor f(ê) can be plotted for various values of $^{eff}L/r$.

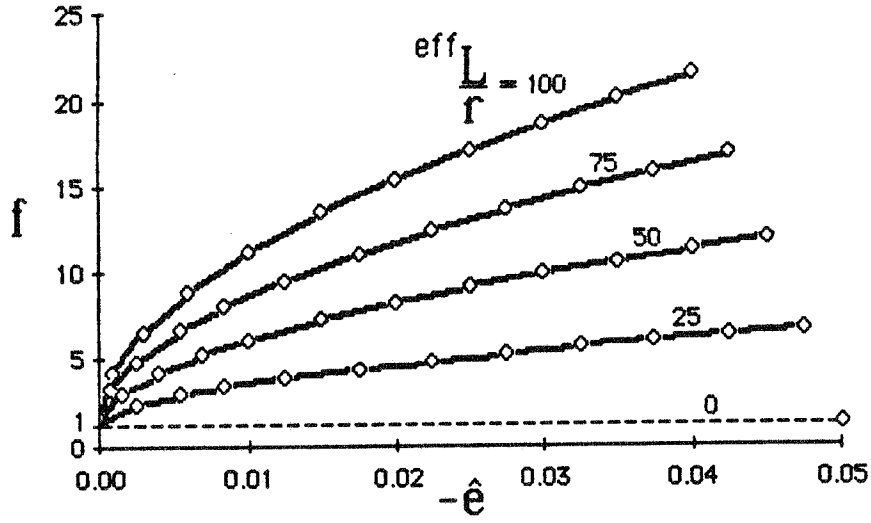

Figure 3.5 Post-Buckling Stress Amplification Factor.

The general implication of the amplification factor curves is that for slender members, where a low stress will cause buckling, there is a high amplification of the stresses once bending starts to occur. This effect is also important for relatively thick members, up to a limiting slenderness where beam theory no longer applies.

Typical members found in space truss structures have values of $^{eff}L/r$ in the range of 25 to 100. This means that the stresses attained at buckling may be magnified significantly before equilibrium is re-established. For a typical buckling problem, where the effective strain is 0.03, a member with effective slenderness of 50 would experience an amplification of 9.8 times the Euler stress. This may lead to yielding, in which case the elastic solution provides an incorrect result for the stress. However, since the elastic stiffness is dramatically reduced once buckling occurs, a further reduction due to yielding may be ignored if the structure can distribute the load imbalance to other members. In this case, the elastic solution is valid in the calculation of loads and displacements for practical truss structures.

4. Program Development

The software modules used for the analyses in this project originate from the NISA80 program. Consideration of the potential interface with controller routines, solution procedures, and path following strategies plays a guiding role in the development of the present and proposed versions of NISA.

4.1 NISA - past, present, future

The development of a comprehensive finite element analysis program typically involves years of research. During this time period many people, with many concepts, are usually involved in the production. The well known result of such projects is an integrated chaos of subroutines which somehow provides the desired results.

NONSAP, originating in Berkeley USA, provided a model for the development of NISA at the Institüt für Baustatik der Universität Stuttgart. Memory management was based on the dynamic allocation of segments of one main array to individual arrays. Allocation was done by the individual modules when and where the space was required. This allowed independence of subroutine development and provided a relatively efficient means of dynamic adaptivity for analyses with a variety of elements.

Modifications to existing NISA modules has proved to be time costly and error prone. Incorrect allocation of memory due to false parameter lists, misdimensioning of subarrays, and COMMON block mistakes have prompted the reconstruction of the NISA controller routines. A project has been started which will provide one common data base management system to remove the potential problems associated with memory allocation by each individual subroutine. Finite elements previously used with NISA are incompatible with the new memory management system and will require extensive modifications before they can be applied.

4.2 Path Following Modules in NISA

The present study involved the use of a trial version of NISA which contained several routines steming from [20] and [21]. A variety of arc length procedures, quasi Newton update methods, and line search options were available. These modules were all combined into one group so that they could be compared and improved for their eventual implementation in future versions of NISA. The available arc length procedures included:

1. Updated Normal Plane Iteration [17].
2. Consistently Linearized Iteration [20].
3. Explicit Iteration on Spheres [5].

Choice of the arc length procedure is controlled by the input parameter ICIRC. Depending on the value of this parameter, a search direction is computed using the appropriate formulae. These operations are carried out in the subroutines RIKWEM and CRISFI. The similarity of the arc length formulae has been exploited by Schweizerhof in the computation of updates to provide relatively compact code. Performance of line searches when required is also initiated at this level.

Updates for the stiffness via quasi Newton methods are initiated by specification of a value for the input parameter IBFGS. The value of this parameter is used to globally set the values of a group of logical variables in NISA main. These logical variables can then be manipulated independently of the numbering scheme used as input without requiring alterations throughout successive modules. Solution of the incremental finite element equations is done in subroutine ITERAT. The application of quasi Newton methods is controlled here. Individual lower level routines are called depending on the values of the previously mentioned logical variables.

The procedures implemented in the test versions of NISA can be easily applied in future programs since they are separated into independent modules. Storage locations for intermediate vectors used in the various update formulae are unfortunately allocated as in NISA80 where required. The organization of NISA87 should provide the allocation of memory for these vectors in a more reasonable fashion.

4.3 BTRUSS implementation in NISA

Truss elements found in NISA80 and NONSAP are the predecessors of BTRUSS. The original options for dynamic analysis and initial strain were removed and replaced by yielding and member buckling. The Lagrangian formulation of the stiffness expression was also changed to the Cauchy form. The combination of these alterations required the complete reconstruction of the program module to allow for future implementation into NISA87.

The BTRUSS module is structured in seven parts:

1. Control.
2. Data Management.
3. Option Selection.
4. Data i/o.
5. Stiffness Calculation.
6. Stress Calculation.
7. Material Law.

The control module (BTRUSS) handles all interface with the calling routines. Data management, option selection, data i/o, stiffness and stress calculations are all initiated and organized here, but performed by lower level routines.

Association of data is provided through a simple management routine (DBMGR). All possible COMMON blocks are contained here and values of parameters are passed back to BTRUSS. This should make it easier for the future application of the data aquisition and management tools in place of the blank COMMON block concept of NISA80.

The performance of further operations is dependent upon the current status of a group of parameters. Instead of tracing flags through a module, to see where they are tested and altered (a programmer's nightmare), one module (OPTION) is used to globally organize the logical execution. The available options are:

1.0 Data i/o.
2.1 Linear Stiffness Calculation
2.21 Nonlinear Stiffness Calculation + Effective Load Update
2.21 Only Effective Load Update (quasi Newton procedures)
3.1 Linear Stress Calculation
3.2 Nonlinear Stress Calculation

The first option includes the assembly of data from an input file for the element connectivity and material properties. This is optionally written to tape for restart options (inconsistent with the above concept). The second option provides some flexibility for the solution procedure. Solvers which require the ability to update the effective loads while using the last or other previous stiffnesses (quasi Newton procedures) are accomodated by the two nonlinear options. Stresses can be calculated using the NISA restart option or by directly calling options 3.1 or 3.2 in BTRUSS. The material law is contained in one final distinct module. The problem is first transposed from three dimensions to one. The material law is applied in one dimension and the solution is transformed back to the three dimensional problem. All references to elastic, plastic, and member buckling are in one dimension.

A debug version of BTRUSS was first implemented with NISA80 on 3.3.86. Tests completed up to 8.4.86 showed that it performs the intended operations of data i/o, stiffness and stress calculation successfully.

5. Numerical Examples

The application of path following methods in nonlinear finite element analysis can be demonstrated by the computation of several demanding examples. Initially, a few problems are given to confirm the validity of the results obtained from the BTRUSS element. Several small extremely nonlinear problems provide further tests for the path following procedures. A comprehensive study of a large problem provides the basis for numerical comparison of the various algorithms presently implemented in NISA.

5.1 Test of the BTRUSS Element

Patch tests have been performed which indicate that the element is performing as desired. This includes the elastic, plastic, and buckling modes described in its development. Comparison to the results from other finite element analyses and to theoretical solutions are provided in the following.

Example 1

Numerical solutions for the ultimate elastic behaviour of a shallow two member truss are available from Papadrakakis [14]. The results from this reference, the present study, and hand calculations of the problem are in complete agreement. The solution procedures employed in [14] were the static perturbation and the conjugate gradient techniques. The arc length method was used here. All methods were able to represent the snapping behaviour of this structure.

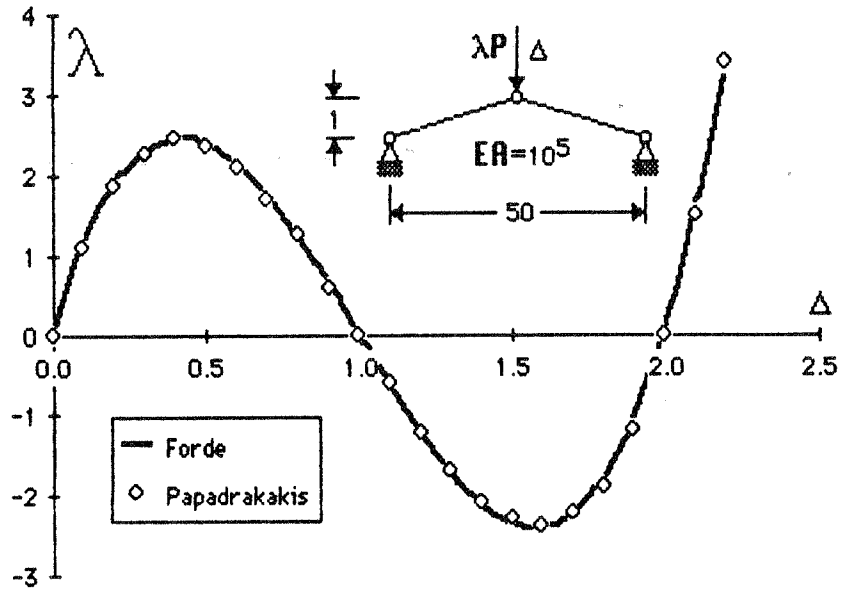

Figure 5.1 Shallow Two Member Truss.

Examples 2 & 3

Simple truss structures, which have theoretical solutions for the initial post buckling behaviour, are available from Britvec[1], and Kondoh/Atluri[12]. The elastic deformation before buckling in both cases is very small, so the buckling loads are essentially as predicted from linear theory. The stress in each element is monitored during the solution procedure allowing the reduction of local stiffness once the critical member buckling stress is attained. Stiffening is observed after large deformations have taken place. Experimental results from Britvec also show the same tendency in the buckled state, indicating that the elastic solution is reasonably accurate.

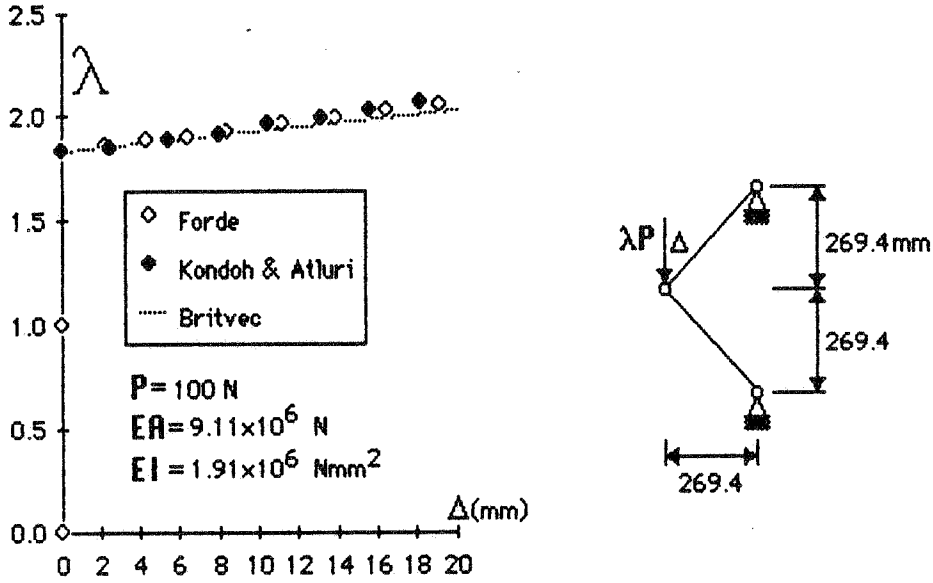

Figure 5.2 Britvec's Truss Structure#1.

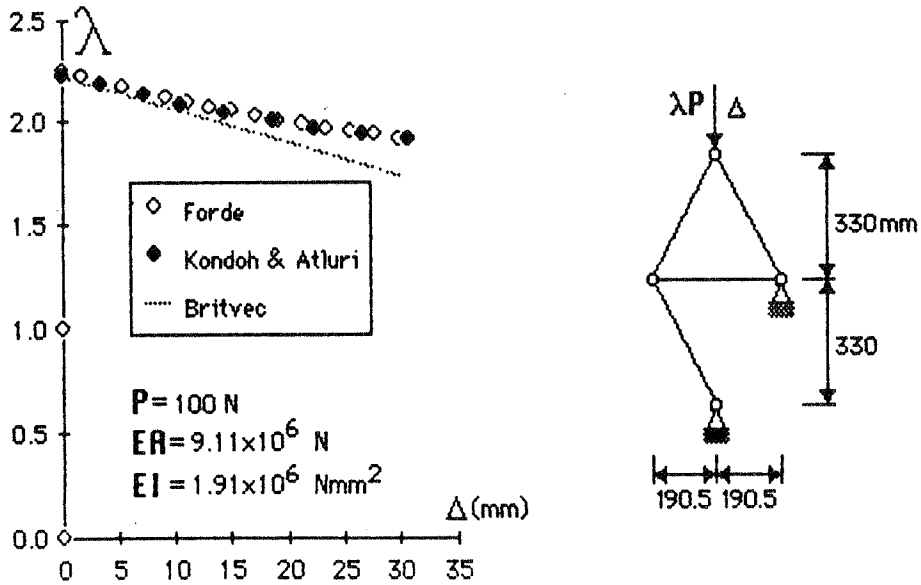

Figure 5.3 Britvec's Truss Structure#2.

5.2 Extremely Nonlinear Problems

Path following procedures can be severely tested in the analysis of small problems. Nonlinearity of the order found there is usually not present in larger structures due to the high degree of indeterminacy. Solution procedures able to handle these small examples can be applied with certainty to the large problems typically found in practice.

Example 4

A shallow arch/suspension system analysed by Powell and Simons [16] combines softening and stiffening behaviour which results in several snaps. This highly nonlinear problem posed no difficulties for all versions of the arc length procedures used in the present analysis.

The results given by [16] are incorrect after the first snap has occured. The correct roots of the load/displacement curve can be calculated directly from geometrical considerations. Equilibrium for $\lambda=0$ occurs in stable (0,2,4) and unstable (1,3) configurations for the following displacements:

0. Initial configuration	(Δ = 0.0)
1. Snap-through of arch system	(Δ = 2.0)
2. Unstrained arch system	(Δ = 4.0)
3. Snap-through of suspension system	(Δ = 4.990)
4. Unstrained suspension system	(Δ = 5.708)

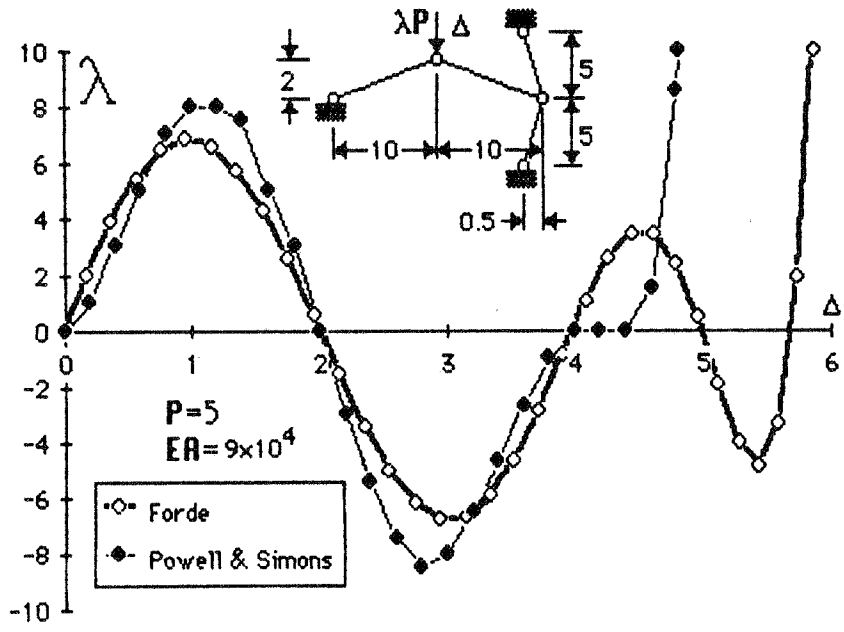

Figure 5.4 Arch/Suspension System.

Example 5

This arch truss was originally analyzed by Powell and Simons [16] using a displacement control technique, and later by Tan [23] using an extrapolated stiffness strategy. Extremely complex behaviour is displayed at the point where snap-through occurs. Controlling the vertical displacement of node 9 leads to failure (since the load/displacement curve is not distinct at $\Delta \approx 8.0$). The same approach with node 13 provides the solution without problem since this displacement increases monotonically. Since the change in direction of the displacement of node 9 is so radical, arc length procedures also experienced difficulty. Explicit iteration on spheres using Crisfield's method combined with BFGS updates was the only procedure able to investigate the behaviour at this point. Other arc length procedures were successfully able to skip over this limit by using a larger arc length.

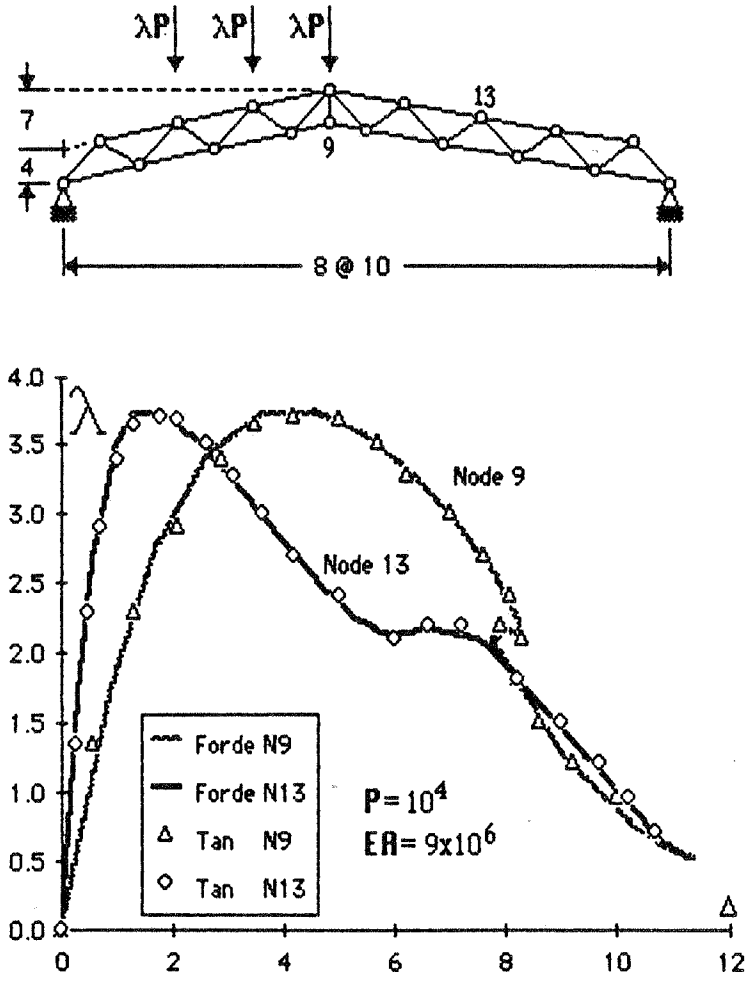

Figure 5.5 Shallow Arch with Complex Behaviour.

Example 6

A 24 member shallow dome structure has been analysed by Paradiso [15] Jagannathan [11], and Papadrakakis [14]. As pointed out by [14] the results of [11] are erroneous due to the missatisfaction of essential geometric constraints at the snap-through. The present study agrees completely with the results from [14] and [15].

All arc length procedures were able to follow the load/displacement path without difficulties. This is typical of shallow shell stability problems where the snapping behaviour follows a "smooth" curve.

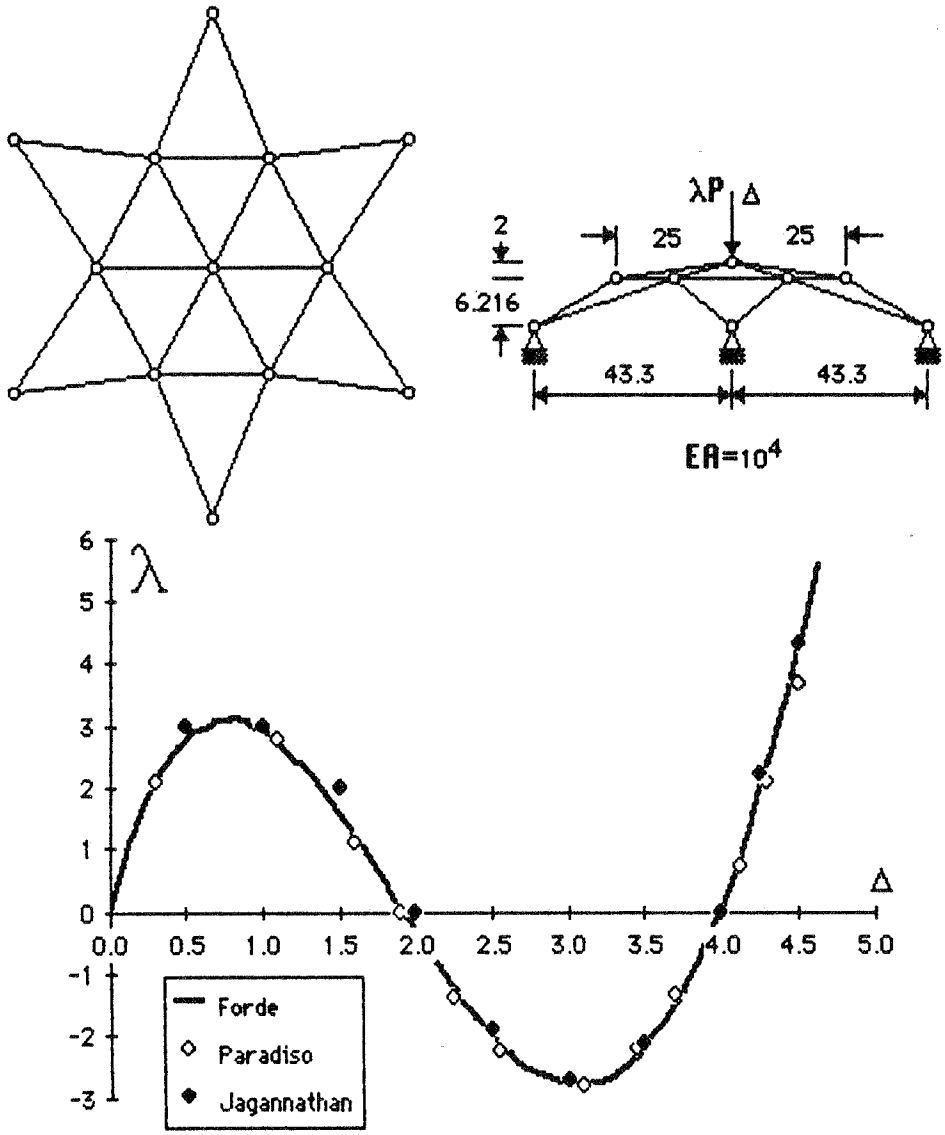

Figure 5.6 Shallow Reticulated Dome.

Example 7

A truss strut structure has been analysed by Thompson and Hunt [24], Rosen and Schmit [19], and Kondoh and Atluri[12]. The present study deals with the influence of local buckling on global instability. Variation of the cross sectional area of key elements introduces an artificial "imperfection" into the structural system. Four cases are chosen as in [12] by defining two member property groups, and then specifying a variety of configurations.

Case	Member buckling	Group 1	Group 2
1	no	1-21	22-35
2	yes	1-21	22-35
3	yes	1-14, 16-21	15, 22-35
4	yes	1-13, 15, 17-21	14,16, 22-35

The natural tendency of the strut structure, owing to its nonsymmetrical geometry, is towards a positive Δ for positive λ. This is amplified in case 3 where the stiffness of member 15 is lowered. Following the same reasoning, this effect is reversed in case 4.

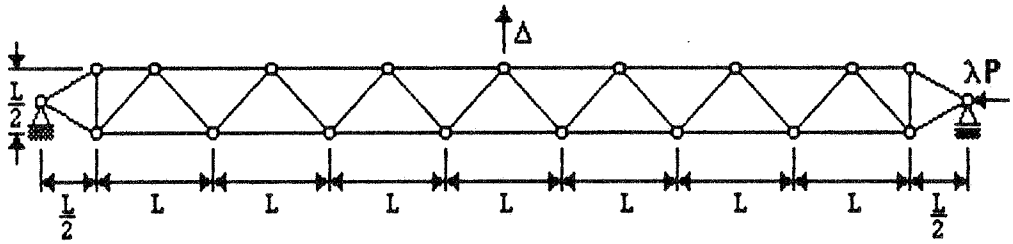

L = 600 mm

$EA_1 = 3.781 \times 10^8$ N P = 1.0×10^6 N

$EA_2 = 3.559 \times 10^8$ N EI = 1.519×10^{11} Nmm^2

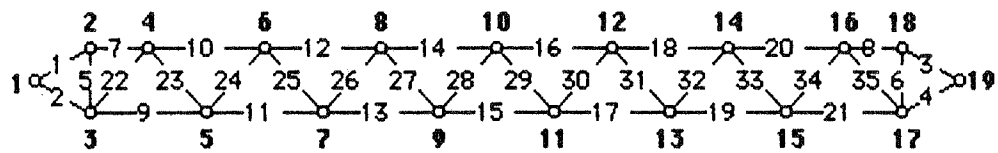

Figure 5.7 Thompson's Strut Structure.

The results from the perfectly elastic case are in complete agreement with the analysis from Kondoh and Atluri [12], however the imperfect structure behaved differently. For a perfect structure, including the effect of member buckling (case 2), a slightly lower ultimate load was obtained. The same ultimate load behaviour was obtained for perfect (case 2) and imperfect (case 3) structures except for in the initial stages of buckling where the imperfection caused additional displacements and an associated critical load reduction. This is more realistic than the results of [12] since the real structure should not be influenced by small imperfections of this type once loaded into the post buckling range.

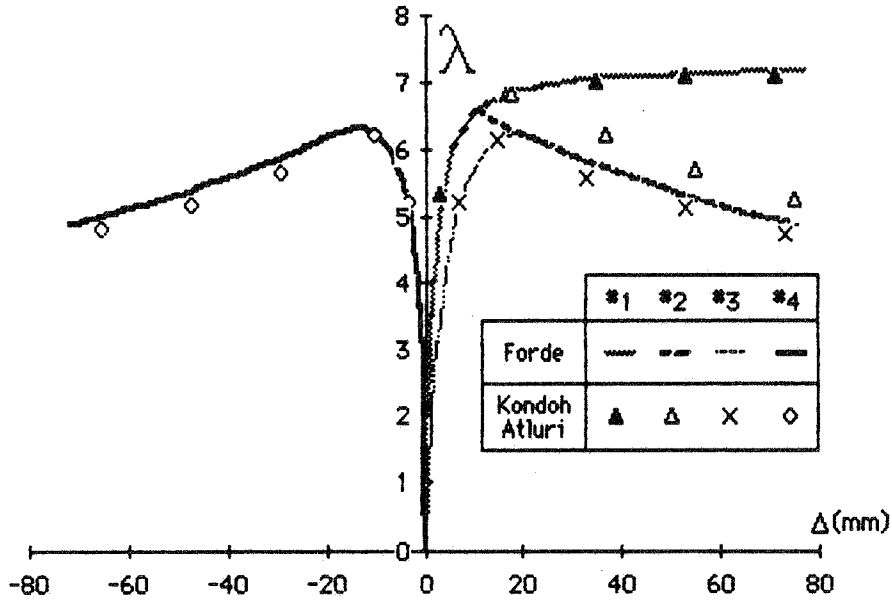

Figure 5.8 Load/Displacement of Thompson's Strut Structure.

The arc length procedures employed had no difficulty in the solution of the problem. Reformation of the stiffness using matrix update methods BFGS, DFP, Broyden, and Davidon all produced equal improvements in convergence at the critical point in case 2. This is the point where local buckling occurs in member 15 and an associated sudden change occurs in the stiffness. This effect is not as prevalent for cases 3 and 4 since the present imperfections cause a more gradual transition at the critical load.

Example 8

An experimental study was performed by Britvec [1] on a reticulated shell structure. Ultimate load capacities were determined for various loading configurations and were compared with theoretical calculations.

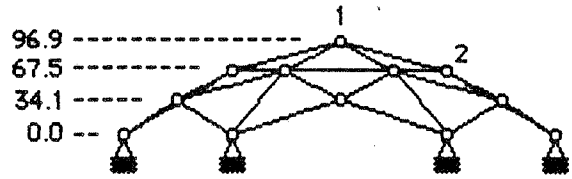

P= 1.00 N ER=1.00x10^6 N EI=8.868x10^4 Nmm^2

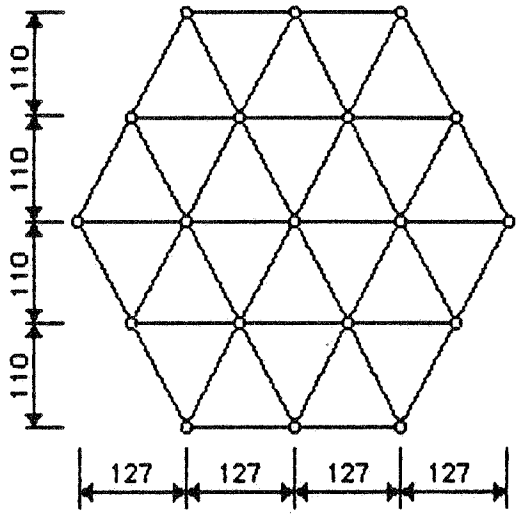

Figure 5.9 Britvec's Experimental Grid Shell.

The results available from Britvec are for two loading cases:

1. One single vertical load at the top of the grid shell.
2. Equal loads at each of the seven upper nodes.

Solution of the elastic problem, excluding member buckling, yields the load/displacement curve for Δ_1 of figure 5.10 (load case #1). The analysis of this problem provided no difficulty for the arc length procedures, however the results are not valid since buckling prevails in the real structure. The incorporation of member buckling into the finite element model provides a realistic solution for the snapping behaviour of the grid shell.

Ultimate Load P_{cr}

Load Case	Britvec Theory	Experiment	Present
1 load	22.96 N	10.80 N	17.01 N
7 loads	67.10 N	40.52 N	69.57 N

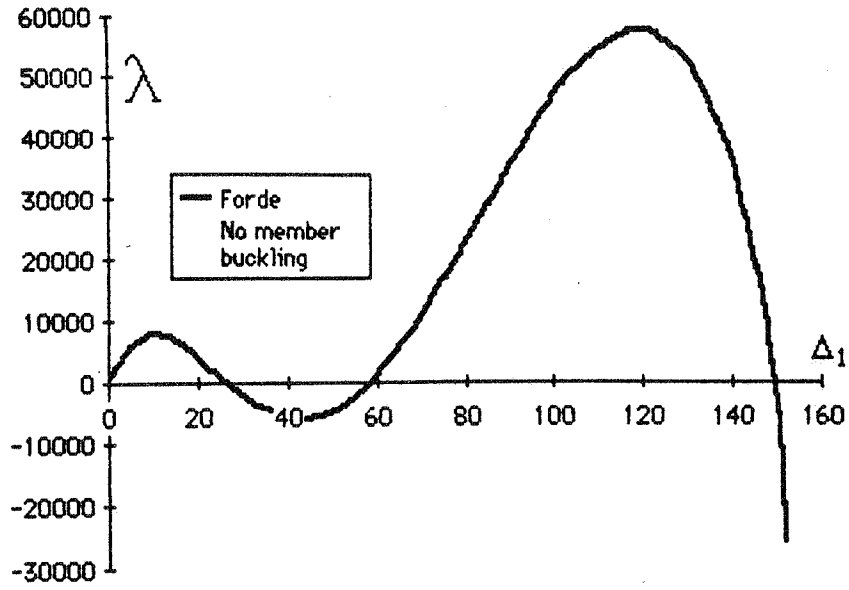

Figure 5.10 Elastic Solution Excluding Member Buckling.

The severe local alteration of the stiffness experienced when the top six members simultaneously buckle (assuming no imperfections are present) causes difficulty for the arc length procedures. If a constant arc length is desired for the complete analysis of the snapping problem, then a relatively large step must be taken at the start. This implies a potential convergence problem at the first step once the stiffness is reformed. Matrix update methods BFGS, DFP, Broyden, and Davidon improved the convergence rate when applied in conjunction with explicit iteration on spheres using Crisfield's method. All other arc length procedures diverged.

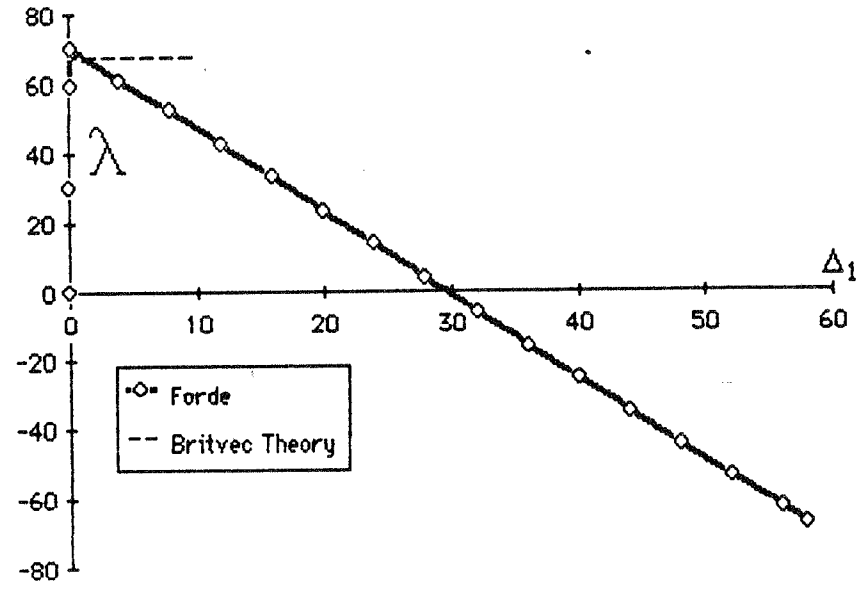

Figure 5.11 Elastic Solution Including Member Buckling.

5.3 Large Nonlinear Problems

Application of path following procedures to the large problems found in engineering practice requires a comprehensive comparison of the various methods. The computational efficiency of the individual formulations can be tested by performing multiple analyses on a relatively demanding structure over a common domain of response.

Example 9

A reticulated shell structure previously analysed by Papadrakakis [14], provides the basis for comparison of the implemented path following procedures in NISA. The complex behaviour of this structure, exemplified by figures 5.13-5.15, is caused by the multiple snapping modes present in the analysis of reticulated shells with many levels. Due to the computational cost associated with the complete problem, the present study deals with only the first snapping mode.

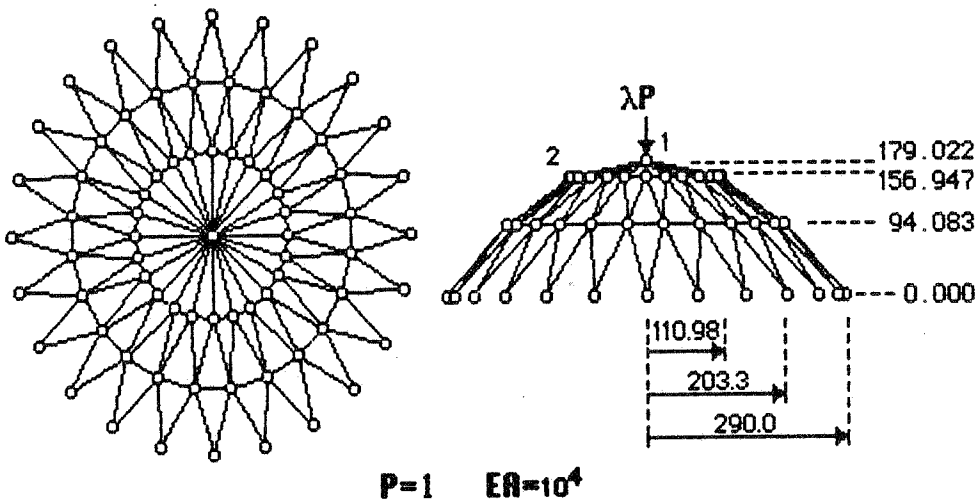

Figure 5.12 Geometry of a Large Reticulated Shell.

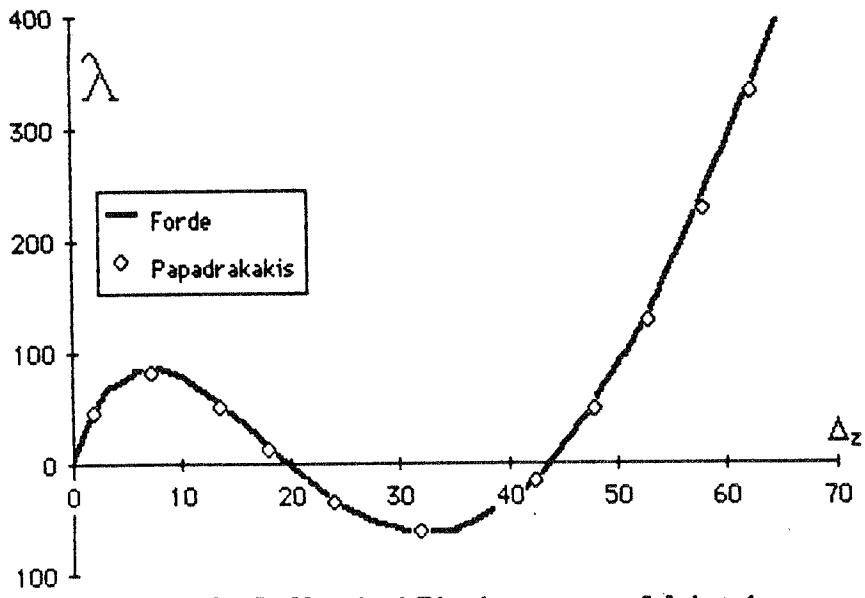

Figure 5.13 Vertical Displacement of Joint 1.

The complex displacement response curves found in this problem provide a typical application for arc length procedures. The results obtained by Papadrakakis agree completely with solutions obtained in the present study. This problem is restricted to elastic behaviour (even though member buckling may be prevalent) simply to provide a means of comparison to an established solution.

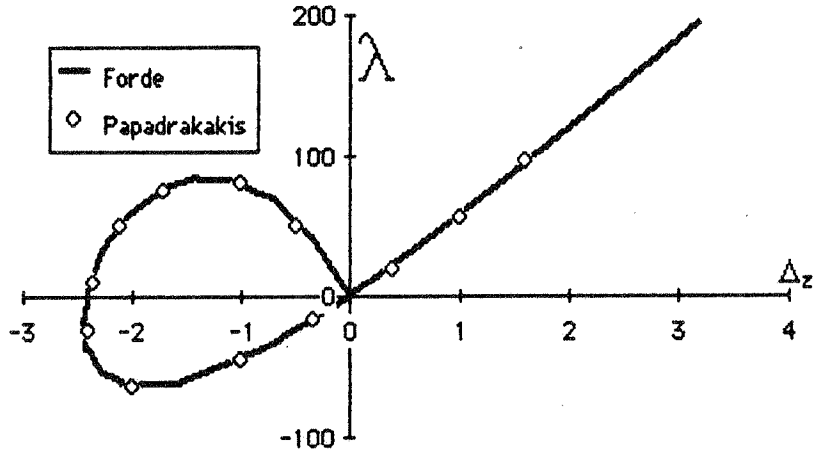

Figure 5.14 Vertical Displacement of Joint 2.

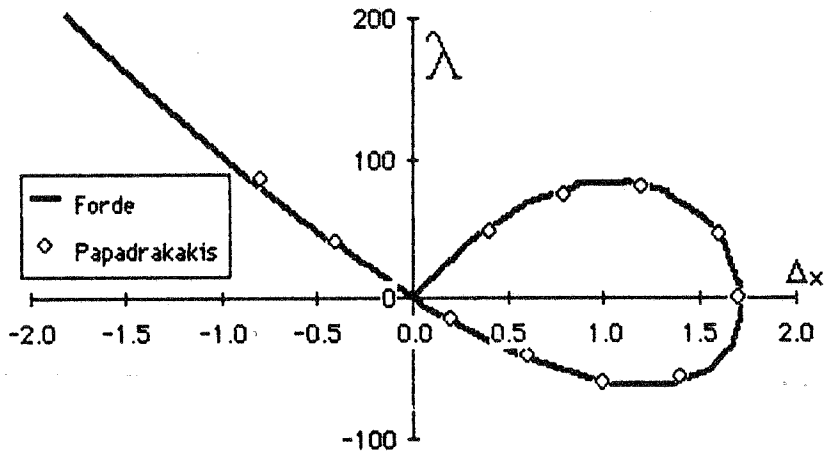

Figure 5.15 Horizontal Displacement of Joint 2.

A variety of analyses were performed using different path following methods. Three arc length procedures were used:

1. Updated Normal Plane Iteration [17].
2. Consistently Linearized Iteration [20].
3. Explicit Iteration on Spheres [5].

Each of these procedures were combined with the quasi Newton methods:

0. No update.
1. BFGS - original form [13].
2. BFGS - product form [13].
3. BFGS - special form [20].
4. Broyden - vector form.
5. Davidon - vector form.
6. DFP - vector form

Two different arc lengths were used, and line searches were alternatively performed, bringing the total number of permutations to 84. The number of iterations required for equilibrium convergence for each arc length step as well as the sum of the iterations and the total CPU time required for computation are listed in tables 5.1 and 5.2.

The results of the analyses indicate that convergence is relatively independent of the applied arc length procedure, however significant variations were observed between the quasi Newton methods. BFGS updates in the special form [20] provided the best overall performance. Ranking the others in terms of this method provides the following ratios:

	Method	N	CPU	Rank
0	No update	1.234	1.036	0
1	BFGS original	1.000	1.092	2
2	BFGS product	1.147	1.159	2
3	BFGS special	1.000	1.000	2
4	Broyden	1.065	1.008	1
5	Davidon	1.082	1.000	1
6	DFP	0.996	1.021	2

N = total number of iterations/total number of iterations for method*3.
CPU = total CPU time/total CPU time for method*3.

The rank two methods, with the exception of the BFGS product form, provided a consistent iteration convergence velocity of approximately 23 percent faster than the traditional modified Newton method. In contrast, the rank one methods provided 15-17 percent improvements. The CPU demand indicates that the original and product formulations for BFGS updates are computationally expensive in comparison to all other methods. Overall convergence behaviour was best with the use of BFGS original and special form rank two updates, followed by Broyden and Davidon rank one updates. Divergence was encountered using the DFP and BFGS product methods in areas of extreme nonlinearity with the use of large arc lengths. Line searches were most effective in case 0 (no update). Otherwise, line searches did not help significantly in terms of iteration convergence nor for CPU demand reduction.

Table 5.1 Analyses with Arc Length = 5.0

	No Line Search: Updated Normal Plane Iteration												Line Search											
	1	2	3	4	5	6	7	8	9	10	Σ	CPU	1	2	3	4	5	6	7	8	9	10	Σ	CPU
0	4	5	5	5	9	6	5	5	5	5	54	4.94	4	5	5	5	9	6	5	5	5	5	54	5.02
1	5	4	5	4	5	5	4	4	4	4	44	5.27	5	4	4	4	5	5	4	4	4	4	43	5.26
2	4	6	4	4	8	5	9	8	4	4	56	5.67	4	6	4	4	5	5	9	9	4	4	54	5.63
3	5	4	5	4	5	5	4	4	4	4	44	4.85	5	4	4	4	5	5	4	4	4	4	43	4.84
4	5	5	5	5	5	5	5	4	4	4	47	4.89	5	5	5	5	5	5	5	4	4	4	47	4.91
5	5	5	5	5	4	4	4	4	4	4	44	4.85	5	5	5	3	4	4	4	4	4	4	42	4.83
6	5	4	5	4	5	5	4	6	4	4	46	4.89	5	4	5	4	5	5	4	6	4	4	46	4.90

	No Line Search: Consistently Linearized Iteration												Line Search											
	1	2	3	4	5	6	7	8	9	10	Σ	CPU	1	2	3	4	5	6	7	8	9	10	Σ	CPU
0	4	5	6	6	6	7	5	5	5	5	54	4.94	4	5	6	6	6	7	5	5	5	5	54	5.03
1	5	4	5	4	4	4	4	5	4	4	43	5.24	5	4	4	4	4	4	4	5	4	4	42	5.22
5	4	6	4	5	4	5	7	8	4	4	51	5.50	4	7	4	5	4	4	7	5	4	4	48	5.42
6	5	4	5	4	4	4	4	5	4	4	43	4.83	5	4	4	4	4	4	4	5	4	4	42	4.82
2	5	5	5	5	5	5	4	4	4	4	46	4.87	5	5	5	5	5	5	4	4	4	4	46	4.88
3	5	5	5	5	5	4	4	4	4	4	45	4.40	5	5	5	5	5	4	4	4	4	4	45	4.90
4	5	4	5	4	4	4	4	5	4	4	43	4.83	5	4	5	4	4	4	4	5	4	4	43	4.84

	No Line Search: Explicit Iteration on Spheres												Line Search											
	1	2	3	4	5	6	7	8	9	10	Σ	CPU	1	2	3	4	5	6	7	8	9	10	Σ	CPU
0	4	5	5	5	8	7	5	5	5	5	54	4.94	4	5	5	5	8	7	5	5	5	5	54	5.03
1	5	4	4	4	5	5	4	4	4	4	43	5.24	5	4	5	4	5	5	4	4	4	4	44	5.29
5	4	6	4	4	5	5	8	8	4	4	52	5.55	4	6	4	4	4	5	8	5	4	4	48	5.43
6	5	4	4	4	5	5	4	4	4	4	43	4.83	5	4	5	4	5	5	4	4	4	4	44	4.86
2	5	5	5	5	5	5	5	4	4	4	47	4.90	5	5	5	5	5	5	5	4	4	4	47	4.91
3	5	5	5	5	4	4	4	4	4	4	44	4.37	5	5	5	5	4	4	4	4	4	4	44	4.87
4	5	4	5	4	5	5	4	5	4	4	45	4.87	5	4	5	4	5	5	4	5	4	4	45	4.88

Table 5.2 Analyses with Arc Length = 10.0

	No Line Search: Updated Normal Plane Iteration												Line Search											
	1	2	3	4	5	6	7	8	9	10	Σ	CPU	1	2	3	4	5	6	7	8	9	10	Σ	CPU
0	5	6	9	8	6	5	5	5	5	5	59	4.82	5	7	7	9	6	5	5	5	5	5	59	4.92
1	5	5	6	5	4	4	4	5	4	4	46	5.13	5	5	6	5	4	4	4	5	4	4	46	5.15
2	-	-	-	-	-	-	-	-	-	-	—	——	-	-	-	-	-	-	-	-	-	-	—	——
3	5	5	6	5	4	4	4	5	4	4	46	4.69	5	5	6	5	4	4	4	5	4	4	46	4.69
4	5	5	6	6	5	4	4	5	5	5	50	4.75	5	5	5	6	5	4	4	5	5	5	49	4.74
5	8	6	7	5	4	5	5	4	4	4	52	4.81	7	6	7	5	4	5	5	4	4	4	51	4.80
6	26	-	-	-	-	-	-	-	-	-	—	——	11	26	-	-	-	-	-	-	-	-	—	——

	No Line Search: Consistently Linearized Iteration												Line Search											
	1	2	3	4	5	6	7	8	9	10	Σ	CPU	1	2	3	4	5	6	7	8	9	10	Σ	CPU
0	6	27	-	-	-	-	-	-	-	-	—	——	6	6	6	6	7	6	5	5	5	5	57	4.90
1	5	6	6	5	5	4	4	4	4	4	47	5.18	5	6	8	5	5	4	4	4	4	4	49	5.27
2	-	-	-	-	-	-	-	-	-	-	—	——	-	-	-	-	-	-	-	-	-	-	—	——
3	5	6	6	5	5	4	4	4	4	4	47	4.71	5	6	8	5	5	4	4	4	4	4	49	4.78
4	5	5	6	5	5	4	4	5	5	5	49	4.73	5	5	6	5	5	4	4	5	5	5	49	4.74
5	7	6	12	6	5	4	4	5	5	4	58	4.93	7	6	13	6	5	4	4	5	4	4	58	4.98
6	20	26	-	-	-	-	-	-	-	-	—	——	26	-	-	-	-	-	-	-	-	-	—	——

	No Line Search: Explicit Iteration on Spheres												Line Search											
	1	2	3	4	5	6	7	8	9	10	Σ	CPU	1	2	3	4	5	6	7	8	9	10	Σ	CPU
0	6	27	-	-	-	-	-	-	-	-	—	——	6	6	6	5	6	6	5	5	5	5	55	4.86
1	5	5	7	4	5	4	4	4	5	4	47	5.17	5	5	5	4	5	4	4	4	5	4	45	5.12
2	-	-	-	-	-	-	-	-	-	-	—	——	-	-	-	-	-	-	-	-	-	-	—	——
3	5	5	7	4	5	4	4	4	5	4	47	4.70	5	5	5	4	5	4	4	4	5	4	45	4.67
4	5	5	5	5	5	4	4	5	5	5	48	4.71	5	5	5	5	5	4	4	5	5	5	48	4.73
5	6	5	7	5	5	4	4	5	5	4	50	4.76	6	5	7	5	5	4	4	5	5	4	50	4.78
6	15	26	-	-	-	-	-	-	-	-	—	——	13	26	-	-	-	-	-	-	-	-	—	——

6. Summary

6.1 Theoretical Results

A derivation of all well known arc length procedures is given using a family of orthogonal plane methods. Various predetermined scalar residuals can be substituted into a general formula to provide updates for normal plane iteration, consistently linearized iteration, and Crisfield's explicit iteration. Based on a theoretical path following example, it was found that convergence velocity is independent of arc length procedures, however the more contrained methods provide better convergence characteristics in the solution of highly nonlinear problems.

Explicitly derived stiffness expressions for space truss elements in elastic, plastic and buckled configurations provide extremely variable local stiffness response. This provides a means of effectively representing the typical stability problems found in reticulated shell structures.

6.2 Numerical Results

As predicted by theory, convergence velocity is relatively independent of arc length procedures, and the more constrained procedures (Crisfield's method and the consistently linearized method) provided better convergence characteristics for the solution of highly nonlinear problems. The use of quasi Newton updates had a large effect on the performance of the arc length procedures. A special form of the BFGS update provided the best results with 23 percent improvement in convergence velocity and 4 percent reduction in computational cost compared to the modified Newton method.

6.3 Recommendations

For the solution of highly nonlinear problems, with severe local alteration of stiffness, the most robust arc length procedure is Crisfield's method. BFGS quasi Newton updates, or pure Newton updates, should be used in conjunction with Crisfield's method to improve convergence velocity and computational efficiency. Other arc length procedures can be used for the solution of less nonlinear problems where convergency is not severely strained. The BFGS special update can again be used to improve the convergence velocity, however it may not provide sufficient computational savings to justify its use under these conditions.

Appendix A

A theoretical comparison of the ability of various arc length procedures to follow the load/displacement curve ($\lambda = A \sin x$) provided the following tables. The convergence criteria was $G^{(i)} < 10^{-4}$. A total of "N" iterations in "m" steps of arc length "s" were performed for each set of parameters.

Modified Newton

Arc Length Method	A	s	m	N	N/m
Normal Planes	1.0	0.5	10	42	4.20
	1.0	1.0	7	46	6.57
	1.0	2.0	*	*	*
	2.0	0.5	10	55	5.50
	2.0	1.0	*	*	*
	2.0	2.0	*	*	*
	3.0	0.5	*	*	*
	3.0	1.0	*	*	*
	3.0	2.0	*	*	*
Updated Planes	1.0	0.5	10	42	4.20
	1.0	1.0	7	46	6.57
	1.0	2.0	4	39	9.75
	2.0	0.5	10	55	5.50
	2.0	1.0	11	74	6.73
	2.0	2.0	*	*	*
	3.0	0.5	*	*	*
	3.0	1.0	*	*	*
	3.0	2.0	*	*	*
Explicit	1.0	0.5	10	41	4.10
	1.0	1.0	7	47	6.71
	1.0	2.0	5	56	11.20
	2.0	0.5	10	55	5.50
	2.0	1.0	10	95	9.50
	2.0	2.0	*	*	*
	3.0	0.5	9	77	8.56
	3.0	1.0	6	104	17.33
	3.0	2.0	*	*	*
Linearized	1.0	0.5	10	41	4.10
	1.0	1.0	7	45	6.43
	1.0	2.0	5	47	9.40
	2.0	0.5	10	56	5.60
	2.0	1.0	10	91	9.10
	2.0	2.0	*	*	*
	3.0	0.5	9	82	9.11
	3.0	1.0	*	*	*
	3.0	2.0	*	*	*
Crisfield	1.0	0.5	10	41	4.10
	1.0	1.0	7	47	6.71
	1.0	2.0	5	56	11.20
	2.0	0.5	10	55	5.50
	2.0	1.0	10	95	9.50
	2.0	2.0	*	*	*
	3.0	0.5	9	77	8.56
	3.0	1.0	6	104	17.33
	3.0	2.0	*	*	*

Pure Newton

Arc Length Method	A	s	m	N	N/m
Normal Planes	1.0	0.5	8	21	2.63
	1.0	1.0	8	34	4.25
	1.0	2.0	*	*	*
	2.0	0.5	6	22	3.67
	2.0	1.0	8	26	3.25
	2.0	2.0	*	*	*
	3.0	0.5	10	31	3.10
	3.0	1.0	*	*	*
	3.0	2.0	*	*	*
Updated Planes	1.0	0.5	8	21	2.63
	1.0	1.0	8	23	2.88
	1.0	2.0	6	22	3.67
	2.0	0.5	8	22	2.75
	2.0	1.0	8	25	3.13
	2.0	2.0	*	*	*
	3.0	0.5	10	28	2.80
	3.0	1.0	*	*	*
	3.0	2.0	*	*	*
Explicit	1.0	0.5	8	21	2.63
	1.0	1.0	8	25	3.13
	1.0	2.0	6	24	4.00
	2.0	0.5	8	23	2.88
	2.0	1.0	8	24	3.00
	2.0	2.0	4	23	5.75
	3.0	0.5	10	29	2.90
	3.0	1.0	*	*	*
	3.0	2.0	4	13	3.25
Linearized	1.0	0.5	8	23	2.88
	1.0	1.0	8	28	3.50
	1.0	2.0	6	23	3.83
	2.0	0.5	8	24	3.00
	2.0	1.0	8	28	3.50
	2.0	2.0	*	*	*
	3.0	0.5	10	29	2.90
	3.0	1.0	*	*	*
	3.0	2.0	*	*	*
Crisfield	1.0	0.5	8	21	2.63
	1.0	1.0	8	25	3.13
	1.0	2.0	6	21	3.50
	2.0	0.5	8	21	2.63
	2.0	1.0	8	24	3.00
	2.0	2.0	4	23	5.75
	3.0	0.5	10	29	2.90
	3.0	1.0	8	23	2.88
	3.0	2.0	4	13	3.25

* divergence (negative discriminant in Crisfield's method).

Appendix B

NISA Input Description for BTRUSS elements

Control Data

- Element Group Control Card C1.1 (one card for each element group)

Column	Variable	Description
1-3	NPAR(1)	Flag for BTRUSS = 1
4-6	NPAR(2)	Number of BTRUSS elements in this group.
46-48	NPAR(16)	Number of different material/section property groups.

Material Data

- Material Group Card C1.2.1 (one for each material group)

Column	Variable	Description
1-5	N	Group number.

- Material Group Card C1.2.2 (one for each material group)

Column	Variable	Description
1-10	E(N)	Young's Modulus.
11-20	AREA(N)	Cross sectional area.
21-30	XINT(N)	Cross sectional inertia.
31-40	SIGPL(N)	Yield stress.
41-50	SIGMAX(N)	Ultimate stress.
51-60	EPSMAX(N)	Ultimate strain.

Element Data

- Element Data Card (one for each element)

Column	Variable	Description
1-5	M	Element number (1 ≤ M ≤ NPAR(2)).
6-10	II	Node at truss end I.
11-15	JJ	Node at truss end J.
16-20	MTYP	Material group (1 ≤ M ≤ NPAR(16)).
21-25	KG	Node generation parameter.

Folgende Berichte sind bereits erschienen:

74-1 M. Becker, J. Bühler, G. Lang-Lendorff, K. Papailiou, J. M. Sättele:
Kontaktkurs EDV im konstruktiven Ingenieurbau.

74-2 G. Werner:
Experimentelle und theoretische Untersuchungen zur Ermittlung des Tragverhaltens biege- und verdrehbeanspruchter Stäbe mit I - Querschnitt.

74-3 K. Tompert:
Berechnung kreiszylindrischer Silos auf elastischer Unterlage.

74-4 W. Riehle:
Studie über verallgemeinerte Variationsfunktionale und ihre Anwendung bei der Methode der finiten Plattenelemente.

75-1 G. Müller, R. W. Rembold, J. M. Sättele, K. H. Schweizerhof, W. Wissmann:
Platten - Theorie, Berechnung, Bemessung. Teil I.

75-2 G. Müller:
Numerische Behandlung der Kirchhoffschen und Reissnerschen Plattentheorie nach einer diskretisierten und erweiterten Trefftz - Methode.

75-3 E. A. Castrillón O.:
Beitrag zur Berechnung langer dünnwandiger dreizelliger Träger unter Berücksichtigung der Profilverformung.

76-1 W. Block, G. Eisenbiegler, R. D. Kugler, H. Lieb, G. Müller, J. Müller, K.-H. Reineck, J. Schlaich, K. H. Schweizerhof, F. Seible:
Platten - Theorie, Berechnung, Bemessung.
Teil II.

76-2 E. Ramm:
Geometrisch nichtlineare Elastostatik und finite Elemente.

77-1 B.-M. Sulke:
Berechnung dünnwandiger prismatischer Faltwerke mit verformbarem mehrzelligen Querschnitt.

78-1 F. Fujii:
Anwendung der Methode der finiten Elemente auf die Berechnung von Stahlbetonplatten.

79-1 B. Brendel:
Geometrisch nichtlineare Elastostabilität.

79-2 H.-G. Berg:
Tragverhalten und Formfindung versteifter Kuppelschalen über quadratischem Grundriß auf Einzelstützen.

79-3 F. W. Bornscheuer, B. Brendel, L. Häfner, E. Ramm, J. M. Sättele:
Fallstudien zu Schalentragwerken (in englischer Sprache).

80-1 R. I. Del Gaizo:
Liegende zylindrische Behälter und Rohre auf Sattellagern endlicher Breite.

80-2 R. W. Rembold:
Beitrag zum Tragverhalten ausgewählter Plattentragwerke unter Berücksichtigung der Reissnerschen Theorie und der Methode der gemischten finiten Elemente.

80-3 J. M. Sättele:
Ein finites Elementkonzept zur Berechnung von Platten und Schalen bei stofflicher und geometrischer Nichtlinearität.

82-1 L. Häfner:
Einfluß einer Rundschweißnaht auf die Stabilität und Traglast des axialbelasteten Kreiszylinders.

82-2 K. Schweizerhof:
Nichtlineare Berechnung von Tragwerken unter verformungsabhängiger Belastung mit finiten Elementen.

82-3 H.-P. Andrä:
Zum Tragverhalten des Auflagerbereichs von Flachdecken.

1 (1983) P. Osterrieder:
Traglastberechnung von räumlichen Stabwerken bei großen Verformungen mit finiten Elementen.

2 (1983) T. A. Kompfner:
Ein finites Elementmodell für die geometrisch und physikalisch nichtlineare Berechnung von Stahlbetonschalen.

3 (1983) A. Diack:
Beitrag zur Stabilität diskret längsversteifter Kreiszylinderschalen unter Axialdruck.

4 (1984) A. Burmeister, F.W. Bornscheuer, E. Ramm:
Traglasten von Kugelbehältern mit Stutzen und Formabweichungen unter Innendruck und Stutzenlängskraft.

Folgende Mitteilungshefte sind bereits erschienen:

84 - 1 Programmbeschreibung NISA 80.
H. Stegmüller, L. Häfner, E. Ramm, J.M. Sättele

84 - 2 Modellierungsfragen - Microcomputer - Erdbebenberechnungen.
A. Burmeister, S. Kimmich, J. Müller, E. Ramm, K. Schweizerhof, H. Stegmüller.

84 - 3 Nonlinear Analysis of Shell-Like Structures.
Nichtlineare Berechnung von Schalentragwerken.
(in englischer Sprache)
T.A. Kompfner, E. Ramm, K. Schweizerhof.

84 - 4 Stability of Steel Structures.
Stabilität von Stahltragwerken.
(in englischer Sprache)
F.W. Bornscheuer, A. Diack, P. Osterrieder, E. Ramm, H. Stegmüller.

85 - 5 Konvergenztest von isoparametrischen degenerierten Platten-/Schalenelementen.
K. Schweizerhof, J. Müller, E. Ramm.